JOURNAL OF MORPHOLOGY 262:608–628 (2004)

Pectoral Fin and Girdle Development in the Basal Actinopterygians *Polyodon spathula* and *Acipenser transmontanus*

Marcus C. Davis,[1]* Neil H. Shubin,[1] and Allan Force[2]

[1]*Department of Organismal Biology and Anatomy, University of Chicago, Chicago, Illinois 60637*
[2]*Department of Molecular Genetics, Benaroya Research Institute at Virginia Mason, Seattle, Washington 98101*

ABSTRACT The pectoral fins of Acipenseriformes possess endoskeletons with elements homologous to both the fin radials of teleosts and the limb bones of tetrapods. Here we present a study of pectoral fin development in the North American paddlefish, *Polyodon spathula*, and the white sturgeon, *Acipenser transmontanus*, which reveals that aspects of both teleost and tetrapod endoskeletal patterning mechanisms are present in Acipenseriformes. Those elements considered homologous to teleost radials, the propterygium and the mesopterygial radials, form via subdivision of an initially chondrogenic plate of mesenchymal cells called the endoskeletal disc. In Acipenseriformes, elements homologous to the sarcopterygian metapterygium develop separately from the endoskeletal disc as an outgrowth of the endoskeletal shoulder girdle that extends into the posterior margin of the finbud. As in tetrapods, the elongating metapterygium and the metapterygial radials form in a proximal to distal order as discrete condensations from initially nonchondrogenic mesenchyme. Patterns of variation seen in the Acipenseriform fin also correlate with putative homology: all variants from the "normal" fin bauplan involved the metapterygium and the metapterygial radials alone. The primary factor distinguishing *Polyodon* and *Acipenser* fin development from each other is the composition of the endoskeletal extracellular matrix. Proteoglycans (visualized with Alcian Blue) and Type II collagen (visualized by immunohistochemistry) are secreted in different places within the mesenchymal anlage of the fin elements and girdle and at different developmental times. Acipenseriform pectoral fins differ from the fins of teleosts in the relative contribution of the endoskeleton and dermal rays. The fins of *Polyodon* and *Acipenser* possess elaborate endoskeletons overlapped along their distal margins by dermal lepidotrichia. In contrast, teleost fins generally possess relatively small endoskeletal radials that articulate with the dermal fin skeleton terminally, with little or no proximodistal overlap. J. Morphol. 262:608–628, 2004.

KEY WORDS: *Polyodon*; *Acipenser*; Acipenseriformes; fin development; chondrogenesis; collagen

Understanding the mechanisms underlying vertebrate paired appendage development is a key problem in evolutionary developmental biology. While classical embryological studies in the late 19th and early 20th century incorporated a diversity of chondrichthyans (Mivart, 1879; Balfour, 1881; Goodrich, 1906), lobe-finned fishes (Semon, 1898), and ray-finned fishes (Thacher, 1877; Sewertzoff, 1926; Kryzanovsky, 1927), modern molecular studies of development have been limited to a few derived sarcopterygian (*Mus, Gallus*) and actinopterygian (*Danio*) model organisms. To make sense of developmental patterns seen in these derived taxa requires an understanding of development in phylogenetically basal taxa. Acipenseriformes (sturgeons, paddlefish, and their extinct relatives) are particularly attractive organisms for research on the evolution of development because of their phylogenetic position near the base of extant actinopterygians. Acipenseriformes are represented by 27 extant species (Bemis and Grande, 1999) and a fossil record extending to the Lower Jurassic (Grande et al., 2002). The majority of morphological (Nelson, 1969; Patterson, 1982; Gardiner and Schaeffer, 1989; Bemis et al., 1997; Coates, 1999) and molecular (Lê et al., 1993) phylogenetic hypotheses support Acipenseriformes as the sister clade to a monophyletic Neopterygii consisting of holosteans (*Amia* + gar; sensu Gardiner et al., 1996) plus teleosts. However, recent molecular hypotheses based on insertions and deletions in the coding sequences of nuclear genes (Venkatesh et al., 2001) and mitochondrial genomic data (Inoue et al., 2003) support an alternative topology in which Acipenseriformes and holosteans form a monophyletic group as the sister clade to teleosts. In either phylogenetic scenario, Acipenseriformes remain basal to the Teleostei.

The pectoral fin skeleton of Acipenseriformes provides a morphological intermediate between the de-

Contract grant sponsors: University of Chicago, National Science Foundation (NSF); Contract grant number: 0207721.

*Current address and correspondence to: Marcus C. Davis, UCSF, Department of Anatomy, Campus Box 2711, San Francisco, CA 94143-2711. E-mail: mdavis@itsa.ucsf.edu

Published online 16 September 2004 in
Wiley InterScience (www.interscience.wiley.com)
DOI: 10.1002/jmor.10264

rived pectoral appendages of teleosts and tetrapods. The pectoral fins of sturgeons and paddlefish contain elements considered homologous to both the fin radials of teleosts and the limb skeleton of tetrapods. This pectoral fin bauplan, like that of other basal actinopterygians and many chondrichthyans, can be divided into three distinct regions. These regions were first described by Carl Gegenbaur (1865) and consist of an anterior propterygium, a middle mesopterygium or series of mesopterygial radials, and a posterior metapterygium. This tribasal arrangement is also present in fossils of the earliest gnathostomes (Janvier, 1996). Placoderms, acanthodians, and the majority of fossil and extant chondrichthyans possess pectoral skeletal elements comparable in relative position and shape to the pro-, meso-, and metapterygia of extant taxa (Ørvig, 1962; Denison, 1978; Coates, 1994; Shubin, 1995). However, some Paleozoic elasmobranchs possess numerous unjointed radials anterior to a metapterygium (e.g., *Cladoselache*; Zangerl, 1981) or possess pectoral fin skeletons consisting only of a metapterygium (i.e., the xenacanthid *Hagenoselache*; Hampe and Heidtke, 1997). Likewise, the pectoral fin skeletons of holocephalans consist of two basal elements rather than three (Didier, 1995; Stahl, 1999). Thus, while much of the fossil and comparative evidence support the hypothesis that a tribasal pectoral fin skeleton is a plesiomorphy of the Gnathostomata, a greater understanding of basal chondrichthyan phylogeny is needed before alternative evolutionary scenarios can be discounted.

In contrast to the conserved skeletal patterns of basal gnathostomes, much of extant osteichthyan diversity can be characterized by patterns of endoskeletal loss. The metapterygium was lost in the lineage leading to teleosts. Thus, the radials in the teleost pectoral fin are considered homologous to the propterygium and mesopterygium of basal taxa. Conversely, sarcopterygians (including tetrapods) have lost the pro- and mesopterygium, retaining only the metapterygial skeleton. An alternative evolutionary scenario proposes that the metapterygial fin skeleton is primitive to gnathostomes and that the propterygium and mesopterygium of chondrichthyans and actinopterygians are convergently evolved (Maisey, 1984; Mabee, 2000). This hypothesis would seem to contradict much of the paleontological data, particularly the presence of tribasal fin endoskeletons in placoderms (e.g., *Ctenurella*; Ørvig, 1962), acanthodians (e.g., *Acanthodes*; Coates, 1994), and many basal chondrichthyans. New fossil discoveries of basal gnathostomes and basal osteichthyans will be necessary to test these hypotheses. However, the implications of either scenario are the same. While the skeletons of teleost pectoral fins and tetrapod forelimbs are homologous at the level of endoskeletal radials, teleosts and tetrapods do not share homologous skeletal elements at the level of "individuated" pro-, meso-, and metapterygia. Among osteichthyans, only basal actinopterygians retain the full complement of elements present in non-osteichthyan gnathostomes.

Teleosts and tetrapods have different mechanisms by which the pectoral endoskeleton is patterned during development. In tetrapods, secretion of extracellular matrix components (collagens and proteoglycans) begins concomitant with, or subsequent to, condensation of individual elements. In contrast, the pectoral fin endoskeleton of teleosts begins as a single, plate-like chondrogenic condensation called the endoskeletal disc (Grandel and Schulte-Merker, 1998). This endoskeletal disc then subdivides into individual radials by decomposition of extracellular matrix in the inter-radial mesenchyme. Which of these patterning mechanisms is representative of the primitive gnathostomes condition is equivocal due to the lack of skeletal homology between teleosts fins and tetrapod limbs. Do the mechanisms of endoskeletal patterning observed in teleosts and tetrapods correlate with the homology of the skeletal elements, or do they reflect derived mechanisms specific to teleost and tetrapod development? Only the investigation of appendage development in basal gnathostome taxa can test these possibilities.

The following is an investigation of the normal development of the paired fins in two Acipenseriformes, the North American paddlefish *Polyodon spathula* and the white sturgeon *Acipenser transmontanus* (Fig. 1). This investigation will serve as a basis for comparative studies of gnathostome appendage development as well as for experimental studies utilizing sturgeons and paddlefish as research organisms. The natural history and biogeography of Acipenseriform species has been discussed by previous authors (Grande and Bemis, 1996; Bemis et al., 1997; Findeis, 1997). Reproduction and growth are well documented in sturgeons and paddlefish, due in part to the economic value of their roe, which is sold as caviar. This aquaculture database, coupled with high fecundity (as many as 10,000 eggs per female) make chondrosteans amiable to laboratory studies of embryonic and larval stages. However, sturgeons and paddlefish take several years to reach sexual maturity and do so at a relatively large body size (Dettlaff et al., 1993), precluding Acipenseriformes from captive breeding under normal laboratory settings.

MATERIALS AND METHODS

Aquaculture and Staging

Fertilized eggs of the North American paddlefish, *Polyodon spathula*, were acquired at 5 days postfertilization (dpf) from Osage Catfisheries (Osage Beach, MO). Staging of *Polyodon* is based on Ballard and Needham (1964) and Bemis and Grande (1992). Approximately 3,000 *Polyodon* embryos were hatched in 5-L plastic tanks at a density of <100 eggs per liter. Embryos were raised at a constant temperature of 18.5 ± 0.5°C, pH 7.2 ± 0.7, salinity of 1.0 ± 0.2 ppt, and a diurnal 12-h light/dark cycle. Hatchery water was constantly filtered and recirculated with a

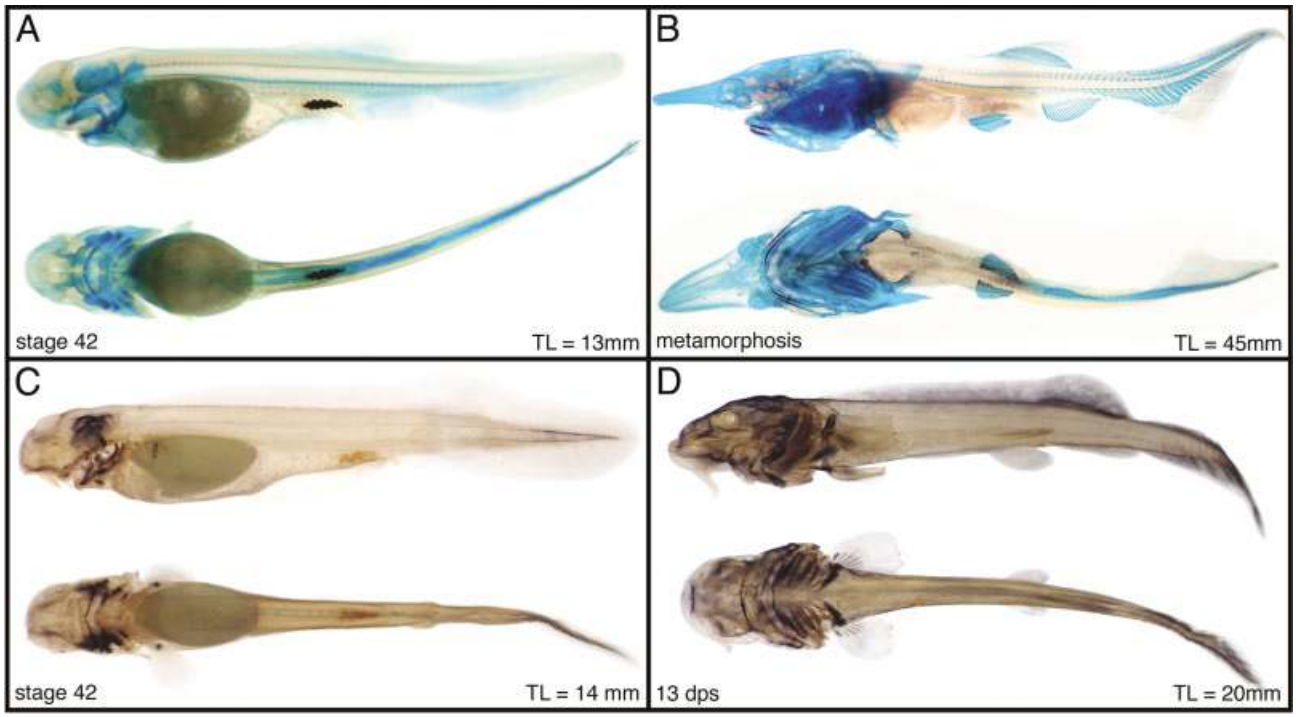

Fig. 1. Survey of *Polyodon spathula* (**A,B**) and *Acipenser transmontanus* (**C,D**) embryos representing developmentally early (**A,C**) and late (**B,D**) stages used in this study. **A:** Stage 42 *P. spathula* stained with Alcian Blue in left lateral (top) and ventral (bottom) view. **B:** Metamorphic (52 days poststaging) *P. spathula* stained with Alcian Blue and Alizarin Red in left lateral (top) and ventral (bottom) view. **C:** Stage 42 *A. transmontanus* immunostained for Type II collagen in left lateral (top) and ventral (bottom) view. **D:** 13 days poststaging *A. transmontanus* immunostained for Type II collagen in left lateral (top) and ventral (bottom) view. Embryos not to scale.

30-min replacement time. All water was filtered through activated charcoal and UV irradiated before returning to the tank. Mortality was low (~3 dead per 1,000 embryos per day) until 1 week after the onset of feeding (21 dpf) when a sharp increase (~25 dead per 1,000 embryos per day) was observed. This mortality spike was primarily due to bites inflicted by other larva. Numerous attacks were observed as well as confirmation of previous reports of larval cannibalism in *Polyodon* (Mims et al., 1999). These problems were most likely density related, as at the time of peak mortality density was high (60 embryos per liter).

Polyodon embryos (n = 40) were sampled at random every 12 h beginning at 6 dpf and continuing until the onset of feeding at stage 46 (15 dpf). At the onset of feeding, larvae (n = 40) were taken every 24 h until 33 dpf. From 33 dpf until metamorphosis (52 dpf) *Polyodon* (n = 20) were sampled every fourth day. Metamorphosis is defined as the point when larvae change feeding mode from the "plucking" of individual prey to filter feeding (sensu Bemis and Grande, 1992). Specimens were labeled by stage with days postfertilization in parentheses until the onset of feeding, after which they were labeled as days poststaging with mean total specimen length in parentheses. Specimen length per stage was determined by taking the mean total length of 10 individuals to the nearest millimeter.

Embryos of the white sturgeon, *Acipenser transmontanus*, were collected in Troutdale, Oregon, by one of us (AF) from a single mating. *Acipenser* embryos (n = 50) were sampled every 24 h between 8 and 31 dpf. As there are no satisfactory staging data for *Acipenser,* specimens were staged based on prelarval development in the Russian sturgeon *Acipenser güldenstädti* (Schmalhausen, 1991; Detlaff et al., 1993). For both species, specimens were labeled by stage with days postfertilization in parentheses until the onset of feeding, after which they were labeled as days poststaging with mean total body length in parentheses. Specimen length per stage was determined by taking the mean total length of 10 individuals to the nearest millimeter.

Fixation

Polyodon were euthanized with a lethal dose of MS-222 (Tricaine). Specimens were fixed for 24 h in 4% paraformaldehyde, dehydrated stepwise into 100% methanol, and stored at 4°C until use. Specimens of *Acipenser* were fixed in 10% neutral buffered formalin and stored in 100% methanol at 4°C.

Alcian Blue Staining

Polyodon (Fig. 1A,B) and *Acipenser* embryos were bleached in 6% hydrogen peroxide/25% methanol in PBT and then stained for proteoglycans with Alcian Blue (0.02% Alcian Blue 8GX/30% glacial acetic acid in anhydrous ethanol; pH adjusted to 2.5). Embryos were destained in 30% glacial acetic acid in anhydrous ethanol and then cleared through a graded ethanol/glycerol series. Specimens were stored in 100% glycerol at 4°C.

Immunochemistry

Embryos of *Polyodon* and *Acipenser* (Fig. 1C,D) were labeled with an antibody against Type II collagen (II-II6B3; acquired from Hybridoma Bank, University of Iowa) using a modification of standard zebrafish immunostaining techniques (Schilling and Kimmel, 1997; Westerfield, 2000). Modifications included serial washing with PBT (PBS media plus 0.2% Tween-20) instead of phosphate buffer, the addition of 0.2% Tween-20 to the blocking solutions, and the use of a biotinylated avidin complex amplifica-

tion step (Vectastain ABC Elite Kit, Vector Laboratories, Burlingame, CA) prior to color development. Signals were developed by diaminobenzidine reaction plus nickel chloride. Stained specimens were graded through an ethanol/glycerol series and stored in 100% glycerol. A minimum of six specimens was immunostained for each developmental stage for both *Polyodon* and *Acipenser*. To support correct interpretation of specimens that lacked staining in the pectoral fins, only specimens that stained positively for Type II collagen in other parts of the embryo were analyzed. Likewise, both whole mount and dissected pectoral fins were immunostained to ensure that antibody penetrance was not an issue.

Histology

Embryos of *Acipenser* were embedded in paraplast following infiltration in xylene and paraplast. Sections (10 μm thickness) were cut on a Microm HM330 rotary microtome. Sections were stained either with hematoxylin and eosin (H&E) or with a trichrome stain that combined H&E and Alcian Blue. For the trichrome stain, slides were soaked in 2 mg/ml 8GX Alcian Blue in glacial acetic acid (pH = 2.5) for 1 min following eosin staining but prior to clearing with xylene. Meyer's H&E were utilized for both staining techniques. Stain slides were preserved with Permount.

Imaging

Specimens were photographed in 100% glycerol using a Nikon D1X digital camera attached to either a Leitz Laborlux S compound microscope for dissected material and sections or a Wild M3C dissecting microscope for whole mounts. Images were edited using Adobe PhotoShop 7.0 (San Jose, CA) for OS X and standardized to absolute white using the "Auto Levels" option.

Terminology

Terminology follows that of Gegenbaur (1865) and Jessen (1972). Additional details of the scapulocoracoid follow Findeis (1997). The dermal skeleton of the pectoral girdle and fin have been described in detail for *Polyodon* (Grande and Bemis, 1991) and for *Acipenser* sp. (Jessen, 1972; Jollie, 1980; Findeis, 1997) and will be discussed only with respect to the girdle and fin endoskeleton.

RESULTS

Polyodon spathula: Pectoral Girdle and Fin Development

Embryos and larva of *Polyodon spathula* were stained with Alcian Blue and immunostained with Type II collagen to investigate pectoral fin and girdle development. Type II collagen immunostaining produced negative results with respect to the pectoral fin and girdle (data not shown). Possible explanations for this result are discussed in the section on variation in the extracellular matrix (below). Figure 1 depicts late embryo (Fig. 1A; Stage 42) and metamorphic (Fig. 1B, total length (TL) = 45 mm) *P. spathula* used in this study. The specific stages used in this study were selected based on the presence of key developmental events not present in previous stages. The pectoral girdles and fins of *P. spathula* were positioned caudoventral and slightly medial to the elongate opercular flaps (Fig. 1A,B). As a result, visualization of the pectoral fins is obscured in whole mount, necessitating dissection of the pectoral girdle and fin prior to imaging (Fig. 2).

Prechondrogenic Stages

The pectoral finbud first appears at Stage 37 (comparable to Ballard and Needham, 1964) as a swelling of the ectoderm on the dorsolateral surface of the yolk sac posterior to the pronephros (data not shown). At Stage 37, the anteroposterior axis of the finbud is parallel to the anteroposterior axis of the body. In subsequent stages the pectoral fins move anteroventrally to a position close to the posterior margin of the opercular flaps. This movement is primarily due to a change in the relative position of the ectoderm ventral to the hypaxial musculature as the yolk sac is depleted rather than the actual migration of the finbud across the ectoderm. At Stages 38 and 39 the finbud consists of the mesenchymal anlage of the shoulder girdle and fin endoskeleton overlaid by the basal stratum and peridermal cells of the ectoderm. During Stages 39 and 40 the apical ectodermal ridge begins to form as a thickening of the basal stratum along the distal margin of the fin.

Stage 42

At Stage 42 (13 days postfertilization, mean TL = 13 mm), Alcian Blue staining first appears in the common anlage of the pectoral fin and girdle (Fig. 2A). Extracellular proteoglycans are present in the chondrogenic condensations of the longitudinal plate of the scapulocoracoid, the presumptive glenoid ridge, and the most proximal regions of the scapular process and metapterygium. The metapterygium is continuous with the shoulder girdle anlage and is a distinct condensation consisting of stacked chondrocytes surrounded by thickened extracellular matrix. In contrast, the finbud mesenchyme anterior and distal to the metapterygium is chondrogenic (stains diffusely with Alcian Blue), but consists of a flattened disc of cells lacking any discernable condensations. This flattened disc of cells averages one or two cells thick dorsoventrally and is histologically comparable to the endoskeletal disc described for *Danio rerio* (Grandel and Schulte-Merker, 1998). Collagenous actinotrichia are not yet visible within the elongating finfold. Globular secretory granules within the epidermis can be seen dotting the fin surface, particularly in the finfold region. Similar vesicles have been described within the pelvic fin epidermis of the rainbow trout *Salmo gairdneri* (Géraudie and Landis, 1982).

Stage 44

At Stage 44 (14 days postfertilization, mean TL = 14 mm), Alcian Blue is visible in the coracoid process with relatively weak staining of the extracellular matrix connecting the coracoid process to the central portion of the scapulocoracoid (arrowhead in Fig.

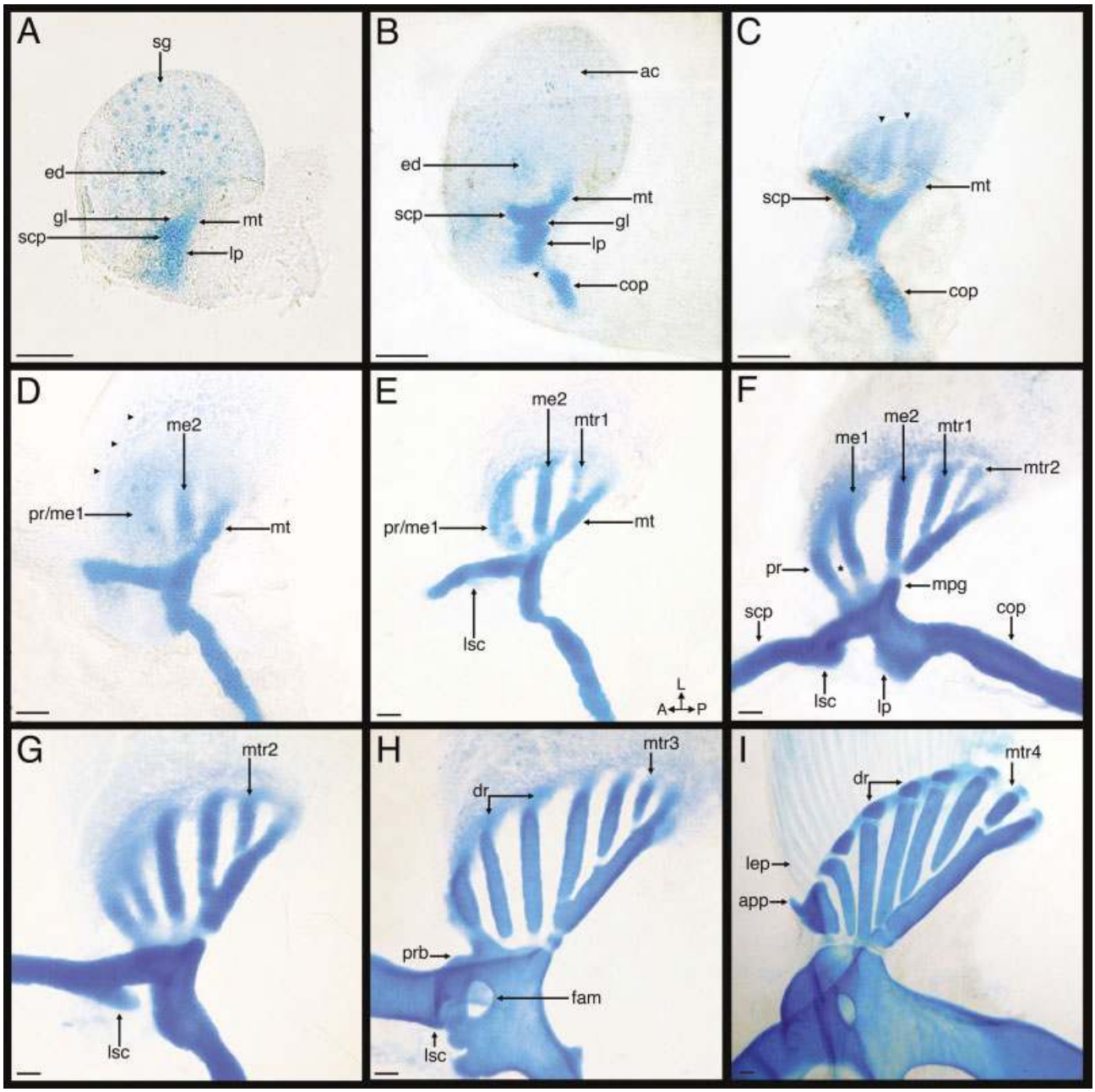

Fig. 2. Developmental series of pectoral fins and girdles of *Polyodon spathula*. Alcian Blue. Fins are shown in dorsal view with girdle in oblique medial view to avoid distortion. Anterior to the left. **A:** Stage 42 (TL = 13 mm). **B:** Stage 44 (TL = 14 mm). Arrowhead denotes connection between the longitudinal plate and the coracoid process. **C:** Stage 45 (TL = 15 mm). **D:** Stage 46 (TL = 17 mm). Arrowheads mark the path of the marginal artery of the fin. **E:** 4 days poststaging (TL = 17 mm). **F:** 10 days poststaging (TL = 18 mm). *Initial subdivision of the common anlage of the propterygium and mesopterygial radial 1. **G:** 16 days poststaging (TL = 19 mm). **H:** 37 days poststaging (TL = 32 mm). **I:** Metamorphosis (52 days poststaging; TL = 45 mm). Scale bars = 100 μm. ac, actinotrichia; app, anterior process of the propterygium; cop, coracoid process; dr, distal radials; ed, endoskeletal disc; gl, glenoid ridge; lep, lepidotrichia; lp, longitudinal plate; lsc, lateral scapular process; ma, marginal artery; me1-2, mesopterygial radials 1 and 2; mpg, metapterygial process of the glenoid; mt, metapterygium; mtr1-4, metapterygial radials 1 through 4; pr, propterygium; pr/me1, common anlage of the propterygium and mesopterygial radial 1, prb, propterygial bridge; scp, scapular process; sg, secretory granules.

2B). This central portion consists of a longitudinal plate ("mittelstück" of Jessen, 1972) connecting the scapular and coracoid processes. The posterior margin of this plate, the glenoid ridge, articulates with the radials in the adult pectoral fin. At Stage 44, the presumptive glenoid ridge area is visible as a small invagination of cells at the base of the metapterygium (Fig. 2B). The scapular process begins to project from the medial margin of the glenoid ridge and the metapterygium continues to elongate pos-

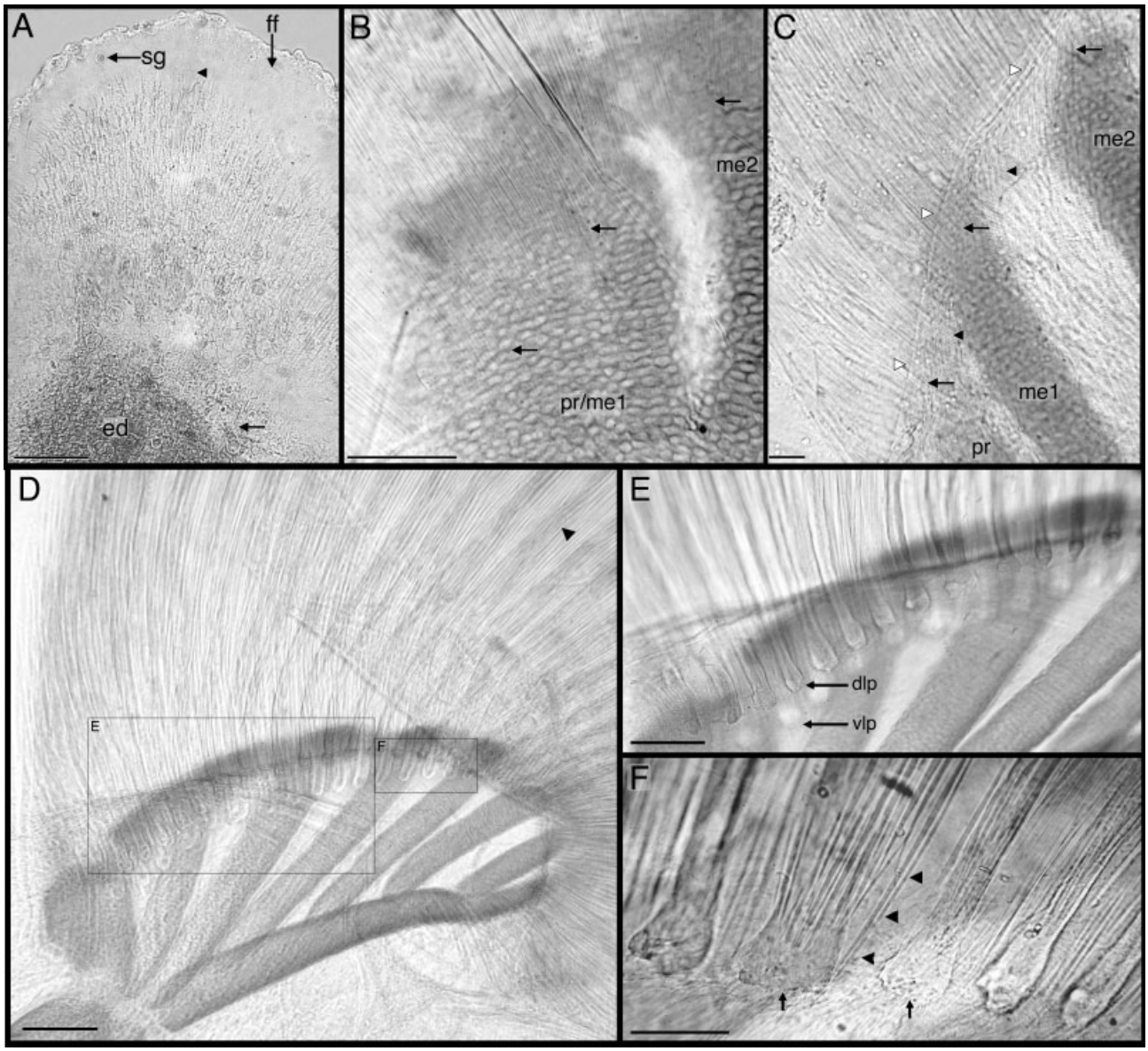

Fig. 3. Development of the dermal fin skeleton in *Polyodon spathula*. Alcian Blue. All specimens shown in dorsal view with anterior to the left. **A:** Stage 44 (TL = 14 mm). Actinotrichia within the finfold can be seen overlapping the distal portion of the endoskeletal disc (arrow) and extending to within 100 μm of the finfold margin (arrowhead). **B:** Stage 46 (TL = 17 mm). Close-up of the anterior radials showing overlap of the actinotrichia (arrows). **C:** 16 days poststaging (TL = 19 mm). Close-up of the anterior radials showing overlap of the actinotrichia (arrows). Muscle fibers (arrowheads) can be seen extending distally to the finbud/finfold junction (open arrowheads). **D:** Metamorphosis (52 days poststaging; TL = 45 mm). Distal radials can be seen within the proximal finfold, overlapped dorsally and ventrally by lepidotrichia. Chondrogenic mesenchyme medial to each hemi-ray stain with Alcian Blue (arrowhead). **E:** Close-up of boxed region in **D** showing asymmetry of overlap of the dorsal and ventral lepidotrichia. **F:** Close-up of boxed region in **D**. Actinotrichia are still present between and medial to the lepidotrichia. Scale bars = 100 μm for **A–D**, 200 μm for **E**, and 400 μm for **F**. dr, distal radial; ed, endoskeletal disc; dlp, dorsal lepidotrichia; ff, finfold; me1-2, mesopterygial radial 1; pr, propterygium; pr/me1, common anlage of the propterygium and mesopterygial radial 1; sg, secretory granule, vlp, ventral lepidotrichia.

terodistally within the finbud. Finbud mesenchyme of the endoskeletal disc stains more intensely than at Stage 42, although condensations are still not present. Stain is absent or weak among cells at the junction between the endoskeletal disc and the glenoid ridge and proximal metapterygium. Actinotrichia are now visible within the finfold (Figs. 2B, 3A). The proximal ends of the actinotrichia overlap the distal margins of the endoskeletal disc (arrow in Fig. 3A). Distally, actinotrichia extend to within 100 μm (arrowhead in Fig. 3A) of the fin margin.

Stage 45

At Stage 45 (15 days postfertilization, mean TL = 15 mm), the scapular and coracoid processes and the

metapterygium continue to elongate distally (Fig. 2C). The endoskeletal disc stains more intensely than at Stage 44, but staining is no longer uniform throughout the disc. Proximodistally oriented zones of weakly stained cells/matrix within the endoskeletal disc mark sites of extracellular proteoglycans decomposition (arrowheads in Fig. 2C). The loss of chondrogenic character within these zones results in subdivision of the endoskeletal disc into individual radials. The first cleared zones to form divide the disc into three chondrogenic regions. The two anterior regions are continuous with the glenoid ridge region of the scapulocoracoid, while cells of the posteriormost region are continuous with the anterior margin of the metapterygium. Diffuse Alcian Blue stain distal to the endoskeletal disc marks chondrogenic mesenchyme adjacent to and within the proximal finfold.

Stage 46

At Stage 46 (16 days postfertilization, mean TL = 17 mm), decomposition of the extracellular matrix within the endoskeletal disc continues (Fig. 2D). The first element to form within the disc, the second mesopterygial radial, is separated from the rest of the endoskeletal disc by widened zones of nonchondrogenic mesenchyme. The anterior mesenchymal anlage will form the propterygium and first mesopterygial radial (Figs. 2D, 3B). The posterior anlage, still continuous with the anterior margin of the metapterygium, will form the first metapterygial radial. The zones of matrix decomposition do not extend into the chondrogenic mesenchyme along the distal periphery of the disc. This distal mesenchyme extends further into the finfold than in previous stages. As a result, the actinotrichia appear to overlap a greater percentage of the developing fin endoskeleton than at earlier stages (compare Fig. 3A,B). The path of the marginal artery can be seen within the finfold and along the anterior margin of the endoskeletal disc (arrowheads in Fig. 2D).

Four Days Poststaging

By 4 days after the onset of feeding (20 days postfertilization, mean TL = 17 mm), decomposition of the chondrogenic extracellular matrix components surrounding the mesopterygial radial 2 is complete (Fig. 2E). At this stage, matrix decomposition at the center of the common anlagen of the propterygium and mesopterygial radial 1 begins. The first metapterygial radial forms by decomposition of matrix between the posterior margin of the developing radial and the anterior margin of the metapterygium. Metapterygial radial 1 remains connected to the metapterygium proximally. Likewise, the developing propterygium, mesopterygial radials, and metapterygium remain connected to the pectoral girdle anlagen at the glenoid ridge. The metapterygium now extends distally to the arch of diffusely stained mesenchyme along the distal periphery of the radials. Stained mesenchyme along the anterior margin of the scapular process marks the formation of the lateral scapular process (Fig. 2E).

Ten Days Poststaging

By 10 days after the onset of feeding (26 days postfertilization, mean TL = 18 mm), the propterygium and first mesopterygial radial are separated by a strip of nonchondrogenic cells (see * in Fig. 2F). Metapterygial radial 2 begins to condense within the zone of nonchondrogenic mesenchyme separating metapterygial radial 1 and the anterior margin of the metapterygium. The first signs of joint formation between the glenoid ridge and the radials appear at 10 days poststaging, as the extracellular matrix in the presumptive joint region stains weakly. Despite the breakdown of extracellular proteoglycans in the joint region, cells in this area retain the stacked morphology of chondrogenic condensations. The medial margin of the glenoid ridge, still continuous with the metapterygium at this stage, expands posterodistally into a prominent metapterygial process of the glenoid (Fig. 2F). The scapular and coracoid processes continue to elongate and increase in overall size. The lateral scapular process begins to elongate toward the anterior margin of the scapulocoracoid plate, which has broadened anteroposteriorly relative to previous stages.

Sixteen Days Poststaging

By 16 days after the onset of feeding (32 days postfertilization, mean TL = 19 mm), metapterygial radial 2 begin to separate from the anterior margin of the metapterygium (Fig. 2G). At this stage, metapterygial radial 1 remains connected to the metapterygium. The propterygium, mesopterygial radials 1 and 2, and the metapterygium remain attached to the glenoid ridge by partially chondrogenic cells. However, the proximal ends of the radials are more rounded, consisting of compact chondrocytes with fewer nonchondrogenic cells connecting the radials to the glenoid ridge. Ventral elongation of the lateral scapular process continues towards the anterior margin of the scapulocoracoid plate. Stain intensity increases in the extracellular matrix along the distal periphery of the finbud, particularly around the distal tips of the radials. Within this chondrogenic band, the distal radials will condense at later stages, concomitant with formation of the lepidotrichia. Actinotrichia (arrows in Fig. 3C) overlap the distal margin of the radials (open arrowheads in Fig. 3C). Under oblique lighting, muscle fibers are visible extending to the distal tips of the radials (arrowheads in Fig. 3C), but are not seen in the presumptive distal radial mesenchyme within the proximal finfold.

Thirty-seven Days Poststaging

At 37 days after the onset of feeding (53 days postfertilization, mean TL = 32 mm), joint formation between the radials and the glenoid ridge is complete or nearly complete (Fig. 2H). The propterygium remains connected by a small number of partially chondrogenic cells to the lateral margin of the glenoid ridge. The metapterygium remains connected to the metapterygial process of the glenoid in 60% of 37 dps specimens analyzed (n = 15). Metapterygial radial 3 has condensed within the nonchondrogenic mesenchyme posterior to the second metapterygial radial. The lateral scapular process has fused to the anterior margin of the scapulocoracoid plate forming the propterygial bridge on which the propterygium pivots. The fusion of the lateral scapular process with the scapulocoracoid plate forms a large foramen bordered by the scapular processes and the glenoid ridge. This foramen accommodates much of the adductor musculature of the pectoral fin (Jessen, 1972) and is likely homologous to the supraglenoid foramen of sarcopterygians (Janvier, 1996). Within the band of Alcian Blue-staining cells distal to the radials, and medial to the proximal margin of the developing fin rays, the distal radials begin to condense. Each distal radial forms as a separate condensation foci distal or slightly posterodistal to an underlying radial. Under oblique lighting, the collagenous prototypes of the lepidotrichia are visible along the anterior margin of the finfold (data not shown).

Metamorphosis (52 Days Poststaging)

At 52 days after the onset of feeding (68 days postfertilization, mean TL = 45 mm), larva reach metamorphosis. By this stage in development the pectoral fin endoskeleton has reached the adult morphology, with a full complement of radials and distal radials (Fig. 2I). The number of metapterygial radials can vary, but the usual complement is four (see discussion regarding variation). The posteriormost metapterygial radial generally articulates with a distal facing process on the metapterygium. Distal radials are condensed, although some chondrogenic mesenchyme remains surrounding the condensations. An anterior process is present on the propterygium that articulates with the lepidotrichia that comprise the leading edge of the finfold. Lepidotrichia overlap the distal radials and the distal ends of the proximal radials (Fig. 3D). The proximodistal overlap of the dermal rays and endoskeletal radials is equal to 6–8% of total fin length at metamorphosis (n = 10). The degree of proximodistal overlap between the lepidotrichia and the radials in adulthood is equivalent to the degree of overlap between actinotrichia and the endoskeletal disc at early stages of pectoral fin development. However, the total amount of endoskeletal/dermal overlap has increased due to the condensation of distal radials within the proximal finfold. There is some asymmetry between dorsal and ventral sets of lepidotrichia, with ventral lepidotrichia overlapping more proximally than do the dorsal lepidotrichia (Fig. 3E). Overlap of the endoskeleton by the lepidotrichia follows the orientation of the actinotrichia (Fig. 3F), with decreasing overlap of more posterior rays (Fig. 3D).

Acipenser transmontanus: Pectoral Girdle and Pectoral Fin Endoskeleton

Embryos and larva of *Acipenser transmontanus* were stained with Alcian Blue and immunostained with Type II collagen to investigate pectoral fin and girdle development. Figure 1 depicts the earliest stage to stain for Type II collagen in the pectoral girdle (Fig. 1C; Stage 42) and the latest larval stage available for this study (Fig. 1D, TL = 20 mm). The specific stages used in this study were selected based on the presence of key developmental events not present in previous stages. The pectoral fins of *A. transmontanus* project laterally from the body and are not obscured by the operculum as in *Polyodon*. This condition allows for unobstructed viewing and imaging of the pectoral girdle and fins in whole mount (Fig. 4).

Prechondrogenic Stages

Pectoral fin development is first visible between Stages 37 and 38 (comparable to *Acipenser güldenstädti* in Schmalhausen, 1991) as a swelling of the ectoderm on the dorsal surface of the yolk sac (data not shown). This swelling is due to local mesenchymal proliferation that will form the common anlagen of the pectoral girdle and pectoral fin endoskeleton. At these early stages the pectoral finbuds are oriented such that the anteroposterior axis of the fin is parallel to the anteroposterior axis of the body. At this point in development the epidermis of the finbud consists of a superficial peridermal layer overlying cells of the basal stratum. By Stage 38, the apical ectodermal ridge is visible as an anteroposteriorly oriented thickening of the basal stratum along the distal margin of the finbud. Between Stages 38 and 39, this apical ridge elongates distally to form the finfold.

Stage 40

At Stage 40 (14 days postfertilization, mean TL = 14 mm), the first chondrogenic condensations are seen in the common anlage of the pectoral girdle and fin (Fig. 4A). The endoskeletal disc has begun to differentiate into separate radials, as evidenced by faint strips of varying stain intensity (arrowheads in Fig. 4A). At Stage 40, the anlage of the scapulocoracoid is continuous with the finbud mesenchyme.

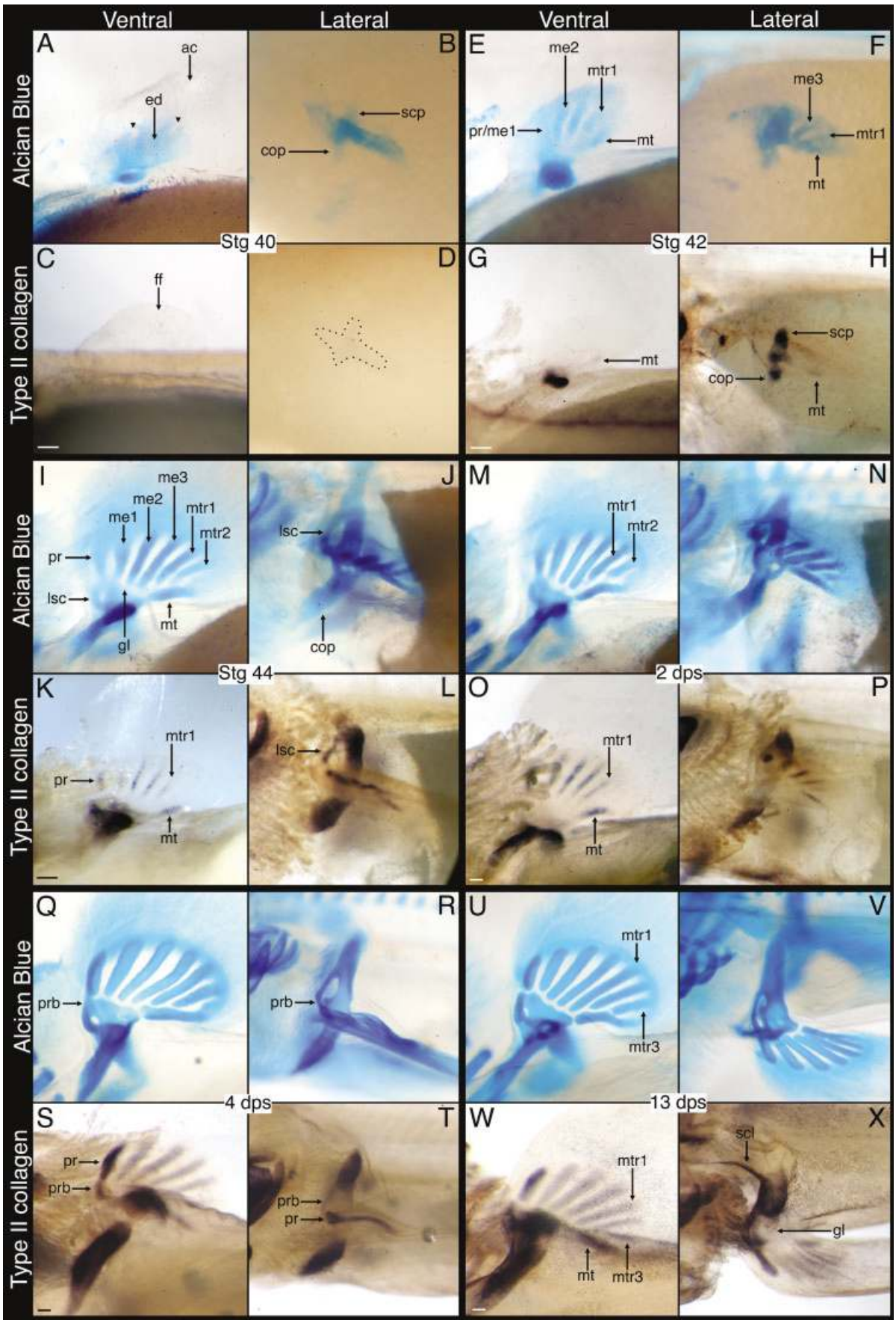
Ventral
Lateral
Ventral
Lateral
Alcian Blue
Type II collagen
A
ac
ed
B
scp
cop
E
me2
mtr1
pr/me1
mt
F
me3
mtr1
mt
Stg 40
Stg 42
C
ff
D
G
mt
H
scp
cop
mt
I
me3
me2
me1
mtr1
mtr2
pr
lsc
gl
mt
J
lsc
cop
M
mtr1
mtr2
N
Stg 44
2 dps
K
mtr1
pr
mt
L
lsc
O
mtr1
mt
P
Q
prb
R
prb
U
mtr1
mtr3
V
4 dps
13 dps
S
pr
prb
T
prb
pr
W
mtr1
mt
mtr3
X
scl
gl

Figure 4

Cells along the dorsal and ventral margins of the longitudinal plate region of the scapulocoracoid begin to condense to form the scapular and coracoid processes, respectively (Fig. 4B). Transverse sections of a Stage 40 fin show that the mesenchyme in the anterior portion of the fin is loosely packed, with only cells with the endoskeletal disc exhibiting the stacked morphology of typical chondrogenic condensations (Fig. 5A). Transverse sections through the presumptive metapterygium show a more compacted and dorsoventrally compressed fin mesenchyme (Fig. 5B). The primary dorsal and ventral musculature of the fin are differentiated by Stage 40 (Fig. 5A,B). Immunostaining detected no Type II collagen in the fin/girdle extracellular matrix at Stages 40 (Fig. 4C,D). Under oblique lighting, collagenous actinotrichia can be seen within the elongating finfold (Fig. 4A).

Stage 42

At Stage 42 (16 days postfertilization, mean TL = 15 mm), the finbud mesenchyme continues to differentiate into separate radials (Figs. 4E,F, 6A). The cells of the endoskeletal are more compacted than at Stage 40 (compare Fig. 5A,C), but are still surrounded by loose mesenchyme. The common anlage of the scapulocoracoid and the metapterygium is visible in anteroposterior (Fig. 5D) and proximodistal section (Fig. 6B,C). The proximal metapterygium is continuous with the glenoid ridge (Fig. 6C,D). The coracoid foramen can be seen piercing the proximal coracoid process just ventral to the glenoid ridge (Fig. 6B–D). As in *Polyodon*, the anterior most condensation consists of the common anlage of the propterygium and mesopterygial radial 1. Mesopterygial radials 2 and 3, the metapterygium, and the first metapterygial radial are also visible in Alcian Blue-stained specimens (Fig. 4E,F) and in section (Fig. 6E,F). The scapulocoracoid is mediolaterally thicker than in previous stages and the scapular and coracoid processes continue to elongate distally (Fig. 4F). By Stage 42, Type II collagen secretion in the extracellular matrix of the shoulder girdle begins (Fig. 4G,H). Stain just dorsal and ventral to the fin base marks the chondrogenic condensations of the scapular and coracoid processes respectively (Fig. 4H). Type II collagen is also present within the longitudinal plate of the scapulocoracoid. However, Type II collagen is absent from the proximal portions of the scapular and coracoid processes where they connect to the longitudinal plate (Fig. 4H). The first Type II collagen secretion in the fin mesenchyme appears between Stages 42 and 43 within the condensation of the metapterygium (Fig. 4H). The finfold and actinotrichia continue to elongate distally.

Stage 44

At Stage 44 (18 days postfertilization, mean TL = 16 mm) the anteriormost anlagen within the fin has divided into the propterygium and mesopterygial radial 1. These two elements remain attached proximally to the anterolateral margin of the glenoid ridge, whereas mesopterygial radials 2 and 3 have separated, as evidenced by the loss of Alcian Blue staining in this area (Fig. 4I). Metapterygial radial 2 is now present and the metapterygium continues to elongate distally. The lateral scapular process begins to condense, connecting the anterior margin of the scapular process (the medial scapular process of Jessen, 1972) to the anterior longitudinal plate (Fig. 4J). Type II collagen is present in the propterygium, mesopterygial radials 1 through 3, and the metapterygial radial 1. At Stage 44, Type II collagen is confined to the core of each developing radial (Fig. 4K). In contrast, extracellular proteoglycans are present throughout the entire condensation (Fig. 4I). Type II collagen and Alcian Blue stain similar portions of the scapular, lateral scapular, and coracoid processes. However, Type II collagen is absent (or present at very low concentrations) from the longitudinal plate and the proximal margins of the scapular and coracoid processes (Fig. 4L).

Two Days Poststaging

Two days after the onset of feeding (20 days postfertilization, mean TL = 18 mm) the mesopterygial radials have separated from the glenoid ridge, while the propterygium remains weakly connected (Fig. 4M). The metapterygium, which is generally the last element to separate from the girdle anlagen, is still partially connected in most specimens at this stage. The metapterygium continues to condense and elongate distally and has developed the distinctive posteromedially oriented bend present in mature specimens of *Acipenser transmontanus* (Fig. 4M). Metapterygial radial 2 continues to condense, although Type II collagen has yet to appear in the core of the condensation (Fig. 4O). Differences in the pattern of extracellular proteoglycans and Type II collagen in the pectoral girdle can be clearly seen in

Fig. 4. Developmental series of pectoral fins and girdles of *Acipenser transmontanus*. Alcian Blue (**A,B,E,F,I,J,M,N,Q, R,U,V**) and immunostained for Type II collagen (**C,D,G,H,K, L,O,P,S,T,W,X**). Whole-mount fins and girdles are shown in ventral (first and third columns) and lateral (second and fourth columns) view. Anterior is to the left. **A–D:** Stage 40 (TL = 14 mm). **E–H:** Stage 42 (TL = 15 mm). **I–L:** Stage 44 (TL = 16 mm). **M–P:** 2 days poststaging (TL = 18 mm). **Q–T:** 4 days poststaging (TL = 18 mm). **U–X:** 13 days poststaging (TL = 20 mm). Scale bars = 100 μm. ac, actinotrichia; cop, coracoid process; ed, endoskeletal disc; ff, finfold; gl, glenoid ridge; lsc, lateral scapular process; me1-3, mesopterygial radials one and three; mt, metapterygium; mtr1-3, metapterygial radials1-3; pr, propterygium; pr/me1, common anlage of the propterygium and mesopterygial radial 1, prb, propterygial bridge; scp, scapular process; scl, supracleithral cartilage.

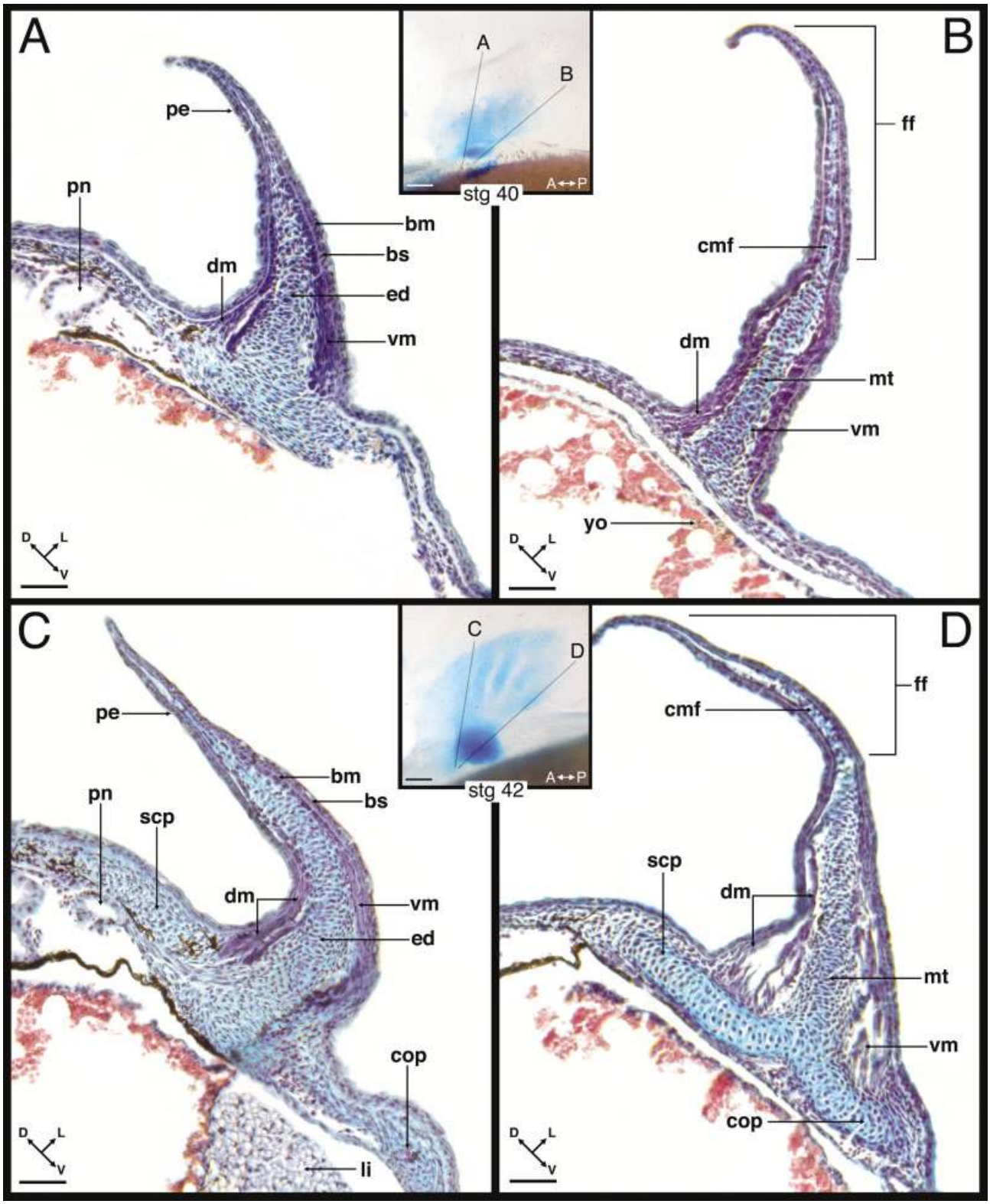

Fig. 5. Pectoral fin and girdle development in *Acipenser transmontanus* at Stage 40 (**A,B**) and Stage 42 (**C,D**) in anteroposterior section. Insets denote plain of section for **A–D**. Hematoxylin-eosin and Alcian Blue trichrome stain. **A:** Larval Stage 40 section through the anterior half of the pectoral fin/girdle at the level of the presumptive propterygium/mesopterygial radial 1. Fin and girdle mesenchyme are loosely packed. **B:** Stage 40 section through the posterior margin of the finbud. Stacked chondrocytes of the metapterygium are visible. **C:** Stage 42 section through the anterior half of the pectoral fin/girdle at the level of the presumptive propterygium/mesopterygial radial 1. Stacked chondrocytes of the endoskeletal disc are visible. **D:** Stage 42 section through the posterior half of the pectoral fin/girdle including the metapterygium showing the common anlage of the scapulocoracoid and metapterygium. Scale bars = 100 μm. All sections 10 μm thick. bm, basement membrane; bs, basal stratum; cmf, chondrogenic mesenchyme in the finfold; cop, coracoid process; dm, dorsal musculature; ed, endoskeletal disc; ff, finfold; li, liver; mt, metapterygium; pe, periderm; pn, pronephros; scp, scapular process; vm, ventral musculature; yo, yolk.

ventrolateral view (Fig. 4N,P). Whereas Alcian Blue staining demonstrates that proteoglycans are ubiquitous throughout the entire girdle anlagen, Type II collagen is limited to the scapular and coracoid processes and is absent from the scapulocoracoid. Likewise, Type II collagen is absent from the proximal portion of the fin radials but is present distally.

Four Days Poststaging

By 4 days after the onset of feeding (22 days postfertilization, mean TL = 18 mm) jointing between the fin endoskeleton and the shoulder girdle is complete (Fig. 4Q). The lateral scapular process and the anterolateral margin of the longitudinal plate meet to form the propterygial bridge (Fig. 4Q). In *Acipenser* the propterygial bridge separates the glenoid ridge from the medial surface of the cleithrum, opening a fossa to accommodate the pectoral musculature that rotates the propterygium and dermal fin spine forward (Findeis, 1997). By 4 days poststaging, Type II collagen is present in the extracellular matrix of all fin radials (Fig. 4S). Type II collagen has expanded beyond the core cells of each radial, but is still absent from the most peripheral cells (compare radial widths in Fig. 4Q,S). The propterygium now stains more intensely for Type II collagen than do the mesopterygial radials or the metapterygium (Fig. 4S), a condition that persists throughout all later stages of *Acipenser transmontanus* available for this study. The pectoral girdle also shows an increase in the intensity of Type II collagen staining (Fig. 4T). However, Type II collagen remains absent in the glenoid ridge, propterygial bridge, and proximalmost regions of the scapular and coracoid processes.

Thirteen Days Poststaging

At 13 days after the onset of feeding (31 days postfertilization, mean TL = 20 mm), the radials of the fin endoskeleton are discrete condensations with defined articulations with the glenoid ridge or anterior margin of the metapterygium (Fig. 4U). In contrast to earlier stages, Type II collagen is present throughout the extracellular matrix of the radials (Fig. 4W). As in previous stages, Type II collagen is absent in the glenoid ridge and longitudinal plate, the proximal portions of the scapular and coracoid processes adjacent to the longitudinal plate, and the proximal region of the metapterygium (Fig. 3X). A strip of Type II collagen staining extending anterodorsally from the anterior margin of the scapular process marks the position of the supracleithral cartilage (Fig. 3X), a unique element found in sturgeons (Acipenseridae, sensu Findeis, 1997) but absent in *Polyodon* and other basal actinopterygians. At 13 days poststaging, lepidotrichial formation has not yet begun, but is likely temporally correlated with distal radial condensation as in *Polyodon spathula* (see above).

DISCUSSION

Skeletal Homology

Phylogenetic analyses and fossil evidence support the hypothesis that a tribasal fin endoskeleton consisting of one or more anterior radials (homologous to the propterygium and/or mesopterygium) and a metapterygium is the primitive condition for gnathostomes (Janvier, 1996; but see Maisey, 1984, for an alternative hypothesis). There are two extant clades of crown-group gnathostomes, chondrichthyans (elasmobranchs + holocephalans) and osteichthyans (sarcopterygians + actinopterygians), and two major extinct clades, acanthodians and placoderms. The phylogenetic relationships of acanthodians and placoderms to the extant clades are uncertain at best (Coates, 1994), although a number of morphological characters support the hypothesis that acanthodians may be the sister-group to Osteichthyes (Maisey, 1986). Acanthodians possess a perichondrally ossified endoskeletal pectoral girdle and mineralized actinotrichia (Denison, 1979). The fin endoskeleton is poorly known in acanthodians and likely remained cartilaginous or possessed a thin perichondrum. In the Permian acanthodian *Acanthodes,* three proximal radials are present (Coates, 1994). The posteriormost radial, presumably the metapterygium, supports two radials articulating with its distal margin. Placoderms were heavily armored gnathostomes mostly endemic to the Devonian period. Like acanthodians, the fin radials of placoderms are poorly known and likely remained cartilaginous or were weakly ossified. The Lower Devonian *Pseudopetalichthys* possesses two proximal radials in the pectoral fin, although the posterior radial appears to consist of two fused elements (Gross, 1962). The pectoral fin endoskeleton of the Upper Devonian *Ctenurella* consists of three proximal elements, the posteriormost being the largest of the three (Ørvig, 1962). The majority of extant and fossil elasmobranch chondrichthyans possess tribasal pectoral fin endoskeletons (Zangerl, 1981; Janvier, 1996), while holocephalans possess dibasal fins (Didier, 1995; Stahl, 1999). Notable exceptions include the multiple unjointed anterior radials of *Cladoselache*, symmoriids, and stethacanthids (Zangerl, 1981), and the monobasal pectoral fins of xenacanthids elasmobranchs and chondrenchelyid holocephalans (Stahl, 1999). In the latter case, the condition likely evolved convergently in xenacanthids and chondrenchelyids in conjunction with a specialized mode of life (Stahl, 1999). A series of anterior radials and a posterior metapterygium are present in stem actinopterygians (e.g., *Mimia* and *Moythomasia*, Gardiner, 1984; *Palaeoniscus*, Jessen, 1972), as well as extant nonteleost actinopterygians. The loss of the metapterygium appears to be

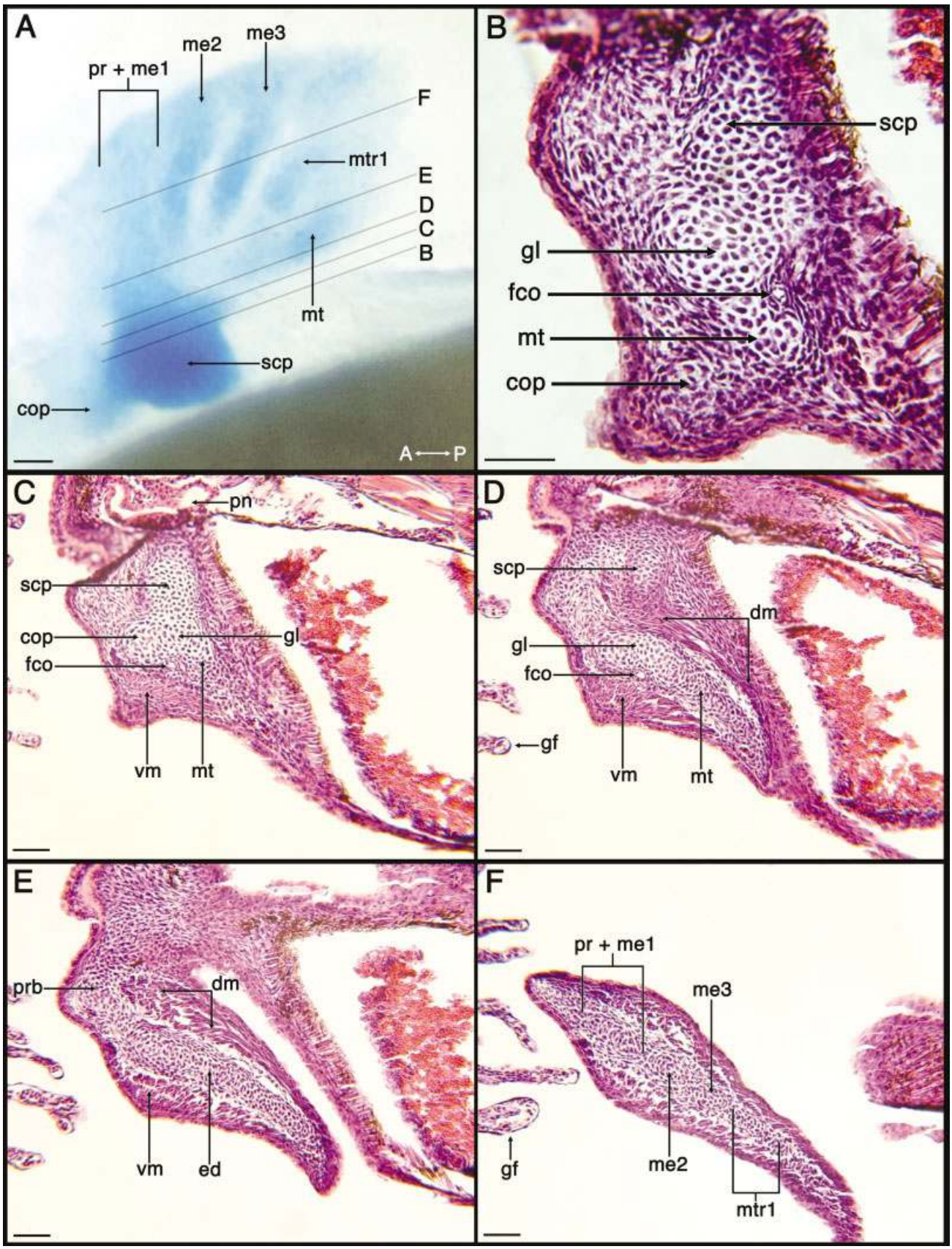
A
me2
me3
pr + me1
F
mtr1
E
D
C
B
mt
scp
cop
A ⟷ P
B
scp
gl
fco
mt
cop
C
pn
scp
cop
gl
fco
vm
mt
D
scp
dm
gl
fco
gf
vm
mt
E
prb
dm
vm
ed
F
pr + me1
me3
gf
me2
mtr1

Figure 6

correlated with the origin of teleosts, although the osteoglossomorph *Hiodon* possesses radials that bifurcate distally (Hilton, 2002) and are similar in morphology to the metapterygium of the nonteleost actinopterygian *Lepisosteus* (MCD, pers. obs.). The total number of radial elements in most teleost pectoral fins rarely exceeds four (Jessen, 1972), although some derived forms may possess as many as 12 radials (De Pinna, 1996). The propterygium of most actinopterygians is perforate (Jessen, 1972), allowing for passage of appendicular vasculature and nerves to the anterior portions of the fin (Janvier, 1996). However, this character is absent in the stem actinopterygians *Cheirolepis* and *Howqualepis* (Long, 1988) and in the extant *Polypterus* and is more accurately a synapomorphy of Actinopteri (sensu Patterson, 1982). Posterior to the propterygium are the mesopterygial radials. Like the propterygium, the mesopterygial radials articulate with the scapulocoracoid proximally.

In actinopterygians, there are two phases of endoskeletal patterning. In the first phase the initially chondrogenic endoskeletal disc subdivides to form individual radials via decomposition of intervening extracellular matrix. In teleosts, secretion of extracellular proteoglycans begins prior to formation of the radials. In the zebrafish *Danio*, proteoglycan secretion is correlated with the formation of the endoskeletal disc at early finbud stages (Grandel and Schulte-Merker, 1998). Other extracellular matrix components, namely Type II collagen, may also be secreted prior to disc subdivision in *Danio* (MCD, pers. obs). The second phase of development involves the condensation of the distal radials. Observations from *Polyodon* development support previous interpretations that distal radials form as discrete condensation foci after endoskeletal disc subdivision (Grandel and Schulte-Merker, 1998) in a manner not unlike carpal/tarsal formation in tetrapods (Shubin and Alberch, 1986). However, signals mediating distal radial formation may involve ectodermal tissues owing to the appearance of the lepidotrichia concomitant with distal radial condensation (see below).

Development of the pectoral endoskeleton in *Polyodon* and *Acipenser* differs from the pattern seen in teleosts in a couple of important ways. At comparable stages, the pectoral fins of teleosts consist of undifferentiated, flattened discs of chondrogenic mesenchyme, while the pectoral fins of Acipenseriformes consist of a similar chondrogenic disc, but one that is attached along its posterior margin to a chondrogenic condensation continuous with the endoskeletal shoulder girdle. Thus, in *Polyodon* and *Acipenser* the metapterygium is already present at the earliest stages of fin development (Figs. 5D, 6B–D) prior to subdivision of the radials (Figs. 2A, 5B). Another important difference between endoskeletal patterning in teleosts and Acipenseriformes is that in *Polyodon* and *Acipenser* some of the radials form after subdivision of the endoskeletal disc. In *Polyodon*, only the first metapterygial radial forms by decomposition of surrounding chondrogenic mesenchyme (although see skeletal variation discussion below). The second, third, and fourth metapterygial radials form as condensation foci within the nonchondrogenic mesenchyme between the first metapterygial radial and the anterior margin of the metapterygium. In this regard, the metapterygial radials form in a manner similar to distal radials or to the limb bones of tetrapods (Shubin and Alberch, 1986) and sarcopterygian fish (Semon, 1898; Joss and Longhurst, 2001). Indeed, the primary morphological difference between the metapterygium of Acipenseriformes and that of sarcopterygians is in the presence of joints along the proximodistal axis (Davis, 2003).

The "composite" fin of *Polyodon* and *Acipenser*, possessing both a teleost-like endoskeletal disc and a sarcopterygian-like metapterygial condensation, has been generally overlooked in previous descriptions of Acipenseriform fin development (Sewertzoff, 1926; Kryzanovsky, 1927; reviewed in Grandel and Schulte-Merker, 1998), although a figure in Kryzanovsky (1927, Abb.16) depicts the metapterygium as a continuous rod connected to the shoulder girdle in larval *Acipenser stellatus*. Interestingly, a condensed metapterygium attached to the flatten endoskeletal disc has also been described for the chondrichthyan *Scyliorhinus canicula* (Balfour, 1881; *Scyllium canicula* of the author). In describing the larval fin endoskeleton in *S. canicula* Balfour writes (bracketed text added for clarity): "The plate [endoskeletal disc] continuous with the basal bar [metapterygium] of the fin is at first, to a considerable extent in the pectoral, and to some extent in the pelvic fin, a continuous lamina, which subsequently segments into rays." A more detailed investigation into fin skeletal patterning in other basal actinopterygians (*Polypterus, Amia*, and *Lepisosteus*) and in Chondrichthyes will be necessary to confirm whether a common scapulocoracoid/metapterygial

Fig. 6. Pectoral fin and girdle development in *Acipenser transmontanus* at Stage 42 in proximodistal section. Anterior is to the left. **A:** Stage 42 whole mount fin and girdle in ventral view as reference for proximodistal sections **B–F**. Sections stained with H&E. **B:** Close-up of the common chondrogenic anlage of the scapulocoracoid and metapterygium. **C:** Common anlage of the scapulocoracoid and metapterygium 40 μm distal to **B**. **D:** Common anlage of the glenoid ridge area and the metapterygium 40 μm distal to **C**. **E:** Section through the proximal endoskeletal disc. **F:** Section through the endoskeletal disc showing the initial condensations of the propterygium and mesopterygial radials. Scale bars = 100 μm. cop, coracoid process; dm, dorsal musculature; ed, endoskeletal disc; fco, coracoid foramen; gf, gill filament; gl, glenoid ridge; lsc, lateral scapular process; me1-3, mesopterygial radials 1-3; mt, metapterygium; mtr1, metapterygial radial 1; pr, propterygium; pr/me1, common anlage of the propterygium and mesopterygial radial 1, prb, propterygial bridge; pn, pronephros; scp, scapular process; vm, ventral musculature

anlage and an anterior endoskeletal disc is an embryonic condition common to all gnathostomes possessing pro-, meso-, and metapterygial radials. However, the developing humerus in *Ambystoma maculatum* larvae forms a continuous condensation with the scapulocoracoid (Burke, 1991), suggesting that a common anlage of the pectoral girdle and the metapterygial axis may be a primitive gnathostome condition.

Thus, the teleost developmental condition is due to loss of the metapterygial axis *and* the early condensation pattern of this element. As a result, the entire fin endoskeleton in teleosts forms via subdivision of the remaining endoskeletal disc. In contrast, sarcopterygians would have lost the pro- and mesopterygial radials and the mechanism by which these elements form. The metapterygial appendage of sarcopterygian fish and tetrapods develops via condensation of elements within a nonchondrogenic mesenchyme. This same mechanism forms the homologous elements in Acipenseriformes, but is not observed during the formation of teleost radials (Mabee and Trendler, 1996; Grandel and Schulte-Merker, 1998). However, the distal radials of teleosts do arise as individual condensation foci (Bouvet, 1968; Grandel and Schulte-Merker, 1998), and may be the skeletal elements most developmentally similar to the sarcopterygian appendage skeleton. Together, these data support the hypothesis that the basal osteichthyan, and possibly gnathostome, condition involved more than one mechanism of endoskeletal patterning within the same fin.

Variation of the Endoskeletal Pattern

Several variant endoskeletal patterns are seen in *Polyodon* and *Acipenser* that differ from the "normal" or most common arrangement (Fig. 7A,D). This variation is confined to the metapterygium and the metapterygial radials, the only common exception being the appearance of an additional mesopterygial radial (Fig. 7B). However, there is a correlation between variation in the number of mesopterygial radials and variation in the number of metapterygial radials in *Polyodon* and *Acipenser*. There are normally two mesopterygial radials in *Polyodon* (Fig. 7D) and the usual complement for *A. transmontanus* is three radials (Fig. 7A). In *Polyodon* there are normally four metapterygial radials articulating with the anterior margin of the metapterygium, while the normal complement in *A. transmontanus* is three. All specimens of *Polyodon* (n = 5; 17% of total) and *Acipenser* (n = 4; 13% of total) scored for the presence of an additional mesopterygial radial possessed one less metapterygial radial than the normal complement. Furthermore, pectoral fins possessing less than the normal complement of mesopterygial radials were never observed. This pattern of variation suggests that supernumerary mesopterygials are due to a "slippage" or a slight shift in the position of the first metapterygial radial. As a result, metapterygial radial 1 lies in articulation with the glenoid ridge instead of the anterior margin of the proximal metapterygium (Fig. 7B). Only one specimen was identified that had fewer than the regular complement of metapterygial radials but had no additional mesopterygial radials, although this condition appeared to be the result of a fusion of metapterygial radials 2 and 3 (arrow in Fig. 7F). However, a specimen of *P. spathula* figured in Grande and Bemis (1991, fig. 21) does lack a metapterygial radial while retaining only two mesopterygial radials. Some specimens possess supernumerary metapterygial radials (Fig. 7E). In these cases, an additional condensation focus appears anterior to the metapterygium and develops into an additional radial.

Another form of variation commonly seen in both *Polyodon* and *Acipenser* is variation of the morphology of the radials. In all but one case such variation was limited to the metapterygium and the metapterygial radials. The one exception was the presence of a novel condensation between a mesopterygial radial and the glenoid ridge (arrow in Fig. 6E). It is interesting to note that this novel condensation was present in a specimen possessing an additional metapterygial radial as well. Other variants observed include bifurcation of the distal end of a radial (Fig. 6C), fusion of adjacent condensation foci (arrow in Fig. 6F), and the presence of partial or complete joints along the metapterygium (arrowhead in Fig. 6F; arrow in Fig. 6G). Joints in the metapterygium are generally located near either the proximal or the distal ends, although joints can appear along mid-length (Grande and Bemis, 1991; see fig. 43 for the Chinese paddlefish *Psephurus gladius*). One specimen of *Polyodon* possessed an additional metapterygial radial articulating with the post-axial side of the metapterygium (arrow in Fig. 6H). This particular condition is reminiscent of the post-axial radials seen in some sarcopterygians (e.g., *Neoceratodus*; Semon, 1898) and in some fossil elasmobranchs (e.g., xenacanthids; Hampe and Heidtke, 1997) and holocephalans (Stahl, 1999).

Variation in the Extracellular Matrix

As mesenchymal cells within the fin/limb bud differentiate into chondrocytes, they begin to synthesize the proteins that will form the extracellular matrix (ECM). Chief among these proteins are cartilage-specific proteoglycans and Type II collagen. The proteoglycans typically found in cartilage can consist of hundreds of glycosaminoglycan chains (usually a mixture of chondrotin sulfate and keratin sulfate chains) covalently linked to a serine-rich core protein (Rodén, 1980). These large proteins are highly hydrophilic, forming hydrated gels that give the ECM of cartilage a swelling pressure that resists compressive forces (Alberts et al., 1983). The most

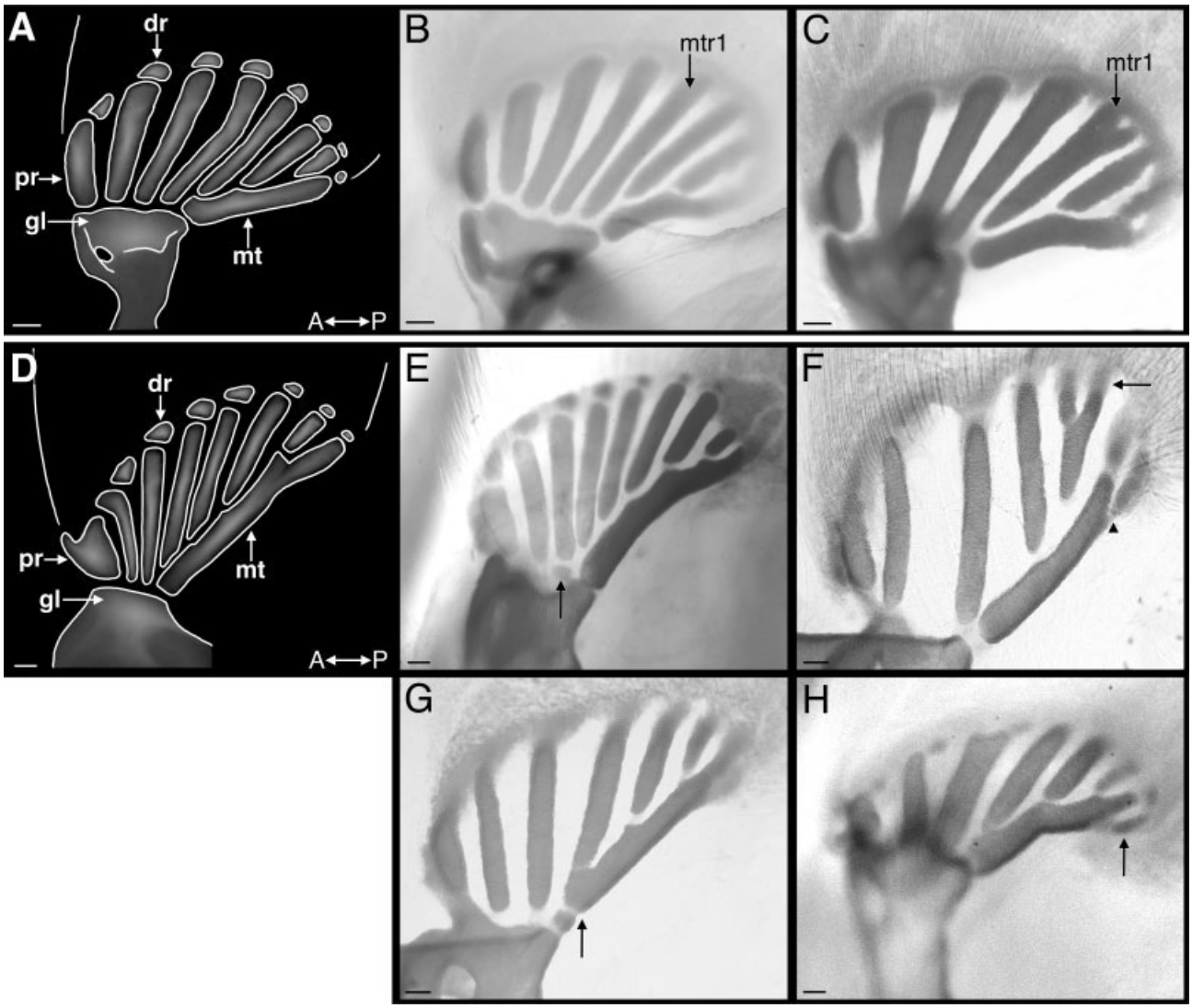

Fig. 7. Variation of the endoskeletal pattern in *Acipenser transmontanus* (**A–C**) and *Polyodon spathula* (**D–H**). Pectoral fins are shown in ventral view for *A. transmontanus* and dorsal view for *P. spathula*. Anterior is to the left. **A:** Illustration of the "normal" fin endoskeleton of *A. transmontanus*. **B:** Slippage of metapterygial radial 1 to articulate with the glenoid ridge instead of with the anterior surface of the metapterygium. **C:** Distal bifurcation of a radial. **D:** Illustration of the "normal" fin endoskeleton of *P. spathula*. **E:** Supernumerary radials. An additional metapterygial radial is present. Arrow denotes a novel condensation between mesopterygial radial 2 and the glenoid ridge. **F:** Distal bifurcation of a radial associated with one less metapterygial radial (arrow). This may involve fusion of the condensations for metapterygial radials 2 and 3. Arrowhead denotes novel joint formation along the metapterygium (compare to **D**). Space between mesopterygial radials 1 and 2 due to distortion of the specimen. **G:** Novel joint or incomplete joint near the base of the metapterygium. This condition is a common variant, scored in 30% of specimens older than 37 days poststaging (TL = 32 mm, n = 30). **H:** Post-axial radial. Scale bars = 100 μm. dr, distal radial; gl, glenoid ridge; mt, metapterygium; mtr1, metapterygial radial 1; pr, propterygium.

abundant proteins in gnathostome ECM are members of the collagen family. The three cartilage specific collagens found in the gnathostome endoskeleton are Types II, IX, and X, with Type II by far the most abundant (Castagnola et al., 1988).

In tetrapods, Type II collagen has been utilized as an earlier marker for chondrogenesis, generally appearing prior to proteoglycan synthesis (Wake and Shubin, 1998). Micromass cultures of mouse limb bud mesenchyme (Edwall-Arvidsson and Wroblewski, 1996) and in vivo studies of chicken mandibular arch condensation (Mina et al., 1991) demonstrate that Type II collagen expression precedes that of cartilage specific proteoglycans. In the endoskeletal disc of zebrafish, proteoglycans (visualized by Alcian Blue) are present by 96 hpf (Grandel and Schulte-Merker, 1998), before detectable levels of Type II collagen are observed (MCD, pers. obs). Type II collagen is first seen in the zebrafish scapulocoracoid (96 hpf) and then throughout the endoskeletal

disc (120 hpf), prior to disc subdivision (MCD, pers. obs.). In *Acipenser* the pattern of Type II expression shows interesting similarities to both tetrapods and zebrafish. As in tetrapods, Type II collagen appears restricted to chondrogenic condensations and not the surrounding mesenchyme. Unlike zebrafish, Type II collagen is not present in the undifferentiated endoskeletal disc (Fig. 4C,G). However, much as in zebrafish, proteoglycans are present in the ECM of the endoskeletal disc prior to accumulation of detectable levels of Type II collagen, the reverse of the condition in tetrapods.

Curiously, Type II collagen was never detected in the glenoid ridge region of the scapulocoracoid in *Acipenser* (Fig. 4P,T,X). This may suggest the presence of other collagens in this region, although monoclonal antibodies for Types I, IX, and XI failed to stain the glenoid ridge (data not shown). Likewise, an alternative monoclonal antibody to Type II collagen (CIIC1) produced similar results to the primary Type II used in this study (II6B3), yet failed to stain the glenoid ridge. In larval Acipenseriformes the glenoid ridge must act as a joint for the moving pectoral fin, even though the condensations of the fin and girdle skeletons remain connected. The functional demands on the glenoid ridge may require a different ECM composition than the rest of the scapulocoracoid. Such variation in ECM composition in cartilage may be the result of biomechanical stimuli (Takahashi et al., 1998; Rabie et al., 2003). The ECM of the glenoid ridge may contain other collagen types not assayed in this study or may possess collagens at concentrations below the sensitivity of standard immunostaining techniques. Alternatively, collagen may be absent from the glenoid ridge altogether. Although collagen is the predominant ECM protein in gnathostome cartilages, the cartilaginous endoskeletons of the extant agnathans *Petromyzon* (lampreys) and *Myxine* (hagfish) are noncollagenous (Robson et al., 2000).

Type II collagen was not observed in the fin endoskeleton of *Polyodon* until late larval stages, and then only in the scapular and coracoid processes and the distal elements of the fin (data not shown). All specimens of *Polyodon* immunostained for Type II collagen stained positively in other parts of the body, primarily the jaws and branchial apparatus. Monoclonal antibodies against Types I, IX, XI, and an alternative Type II collagen failed to stain the fin endoskeleton in *Polyodon*. As in the case of the glenoid ridge of *Acipenser*, either collagens are present that are not recognized by the antibodies available, the concentration of collagen protein is too low to be detected, or portions of the fin endoskeleton in *Polyodon* are composed of noncollagenous cartilage. Cloning and in situ expression of the Type II collagen gene in *Acipenser* and *Polyodon*, as well as upstream genes implicated in the expression of Type II collagen, such as the transcription factor Sox 9 (e.g., Yan et al., 2002), would shed light on these observations.

Development of the Dermal Fin Rays

Actinotrichia comprise the primary structural support of the larval finfolds of *Polyodon* and *Acipenser*. Actinotrichia first appear along the distal margin of the finbud mesenchyme and elongate distally within the developing ectodermal finfold (Fig. 3A). In both taxa the proximal margins of the actinotrichia overlap the distal margin of the endoskeletal disc (arrows in Fig. 3A,B). The actinotrichia along the anterior margin of the finfold overlap the developing endoskeleton more completely than do actinotrichia along the posterior margin, although this is not clearly discernable until later stages (Fig. 3D). A similar pattern of actinotrichial development has been described for the neopterygians *Salmo* (Géraudie and Landis, 1982) and for *Danio* (Grandel and Schulte-Merker, 1998), although in both cases actinotrichia do not appear to overlap the distal margin of the endoskeletal disc, overlapping only the chondrogenic mesenchyme of the presumptive distal radials.

Actinotrichia are composed of elastoidin (Géraudie, 1977), a protein composed of $\alpha 1$ type collagen homotrimers (Kimura et al., 1986). Actinotrichia in both *Acipenser* and *Danio* stain positively for Type I collagen (data not shown), suggesting that elastoidin may crossreact with the antibody for Type I collagen or that the actinotrichia in these taxa may contain Type I collagen (a heterotrimer of $\alpha 1$ and $\alpha 2$ type collagen chains). Previous studies of actinopterygian fin development have observed migration of distal finbud mesenchyme into the finfold concomitant with actinotrichial formation (Géraudie and Landis, 1982; Wood, 1982). Thus, the actinotrichia appear to play a role in organizing mesenchymal invasion of the finfold, perhaps through a mechanism of contact guidance (Wood and Thorogood, 1984). In *Polyodon* and *Acipenser*, mesenchymal invasion of the finfold follows a similar pattern, as evidenced by the appearance of diffuse Alcian Blue within the proximal portions of the finfold shortly after actinotrichia first appear (Figs. 2B, 4A).

The stages of *Acipenser transmontanus* available in this study did not allow for observation of lepidotrichia formation. However, in *Polyodon* lepidotrichia are first visible around 37 days poststaging but do not stain with Alizarin Red until a few days later, suggesting a delay between formation of the collagenous prototype of each ray and subsequent calcification. Jointing of the lepidotrichia first begins in the proximal portions of the each ray, with more anterior lepidotrichia initiating joint formation earliest. Thus, joint formation follows the same general order as lepidotrichial condensation described for *Salmo* (Géraudie and Landis, 1982) and for *Danio*

(Grandel and Schulte-Merker, 1998), starting at the anteroproximal corner of the finfold and proceeding posteriorly and distally. This order of lepidotrichial formation and subsequent jointing appears to be a primitive condition for Osteichthyes. Ontogenetic series of the Devonian fossil sarcopterygian *Eusthenopteron* show that larval specimens possess unjointed lepidotrichia, but that as body length increases jointed lepidotrichia appear (MCD, pers. obs.). Certain osteichthyan groups have convergently lost jointing as well, resulting in elongate rods of bone. The Devonian sarcopterygian *Sauripterus* possesses unjointed lepidotrichia that are unique in their extensive ventral and dorsal overlap of the fin endoskeleton (Davis et al., 2001, 2004). In Syngnathidae (seahorses and pipe fishes), long unjointed demi-rays are present in pectoral and dorsal fins. The loss of ray jointing may reflect specialized locomotor strategies. In *Sauripterus* the unjointed lepidotrichia and their overlap of the fin endoskeleton result in a stiffened appendage that may have been used to push against the substrate or water column (Davis et al., 2004). Likewise, the stiffened demi-rays of syngnathids may reflect the unique locomotor requirements of these fishes (Consi et al., 2001).

Apical Ectodermal Fold and Relative Skeletal Contributions

The relative contribution of the endoskeletal radials and dermal rays to the fin skeleton is one of the key morphological differences between ray-finned and lobe-finned designs (Shubin and Davis, 2004). The general trend is such that actinopterygians possess elaborate dermal fin skeletons with a relatively small endoskeleton, while sarcopterygians possess elongate fin endoskeletons with a lesser contribution to fin surface area from the dermal rays. Teleosts and tetrapods represent the extremes of these conditions, possessing primarily dermal or exclusively endoskeletal appendages, respectively. Phylogenetically basal actinopterygians and sarcopterygians often possess intermediate patterns of dermal and endoskeletal contribution. For example, the pectoral fin skeleton of *Sauripterus* consists of an elaborate endoskeleton sandwiched between massive unjointed dermal rays (Davis et al., 2001, 2004). Such a morphology would not have been predicted by models of paired fin development based on model organisms (Thorogood, 1991; Sordino and Duboule, 1996). In particular, our understanding of the cellular and molecular events behind fin skeletogenesis is based on observations in a few teleosts, particularly *Danio*. In *Danio*, proliferation of finbud mesenchyme ceases when the distally flanking structure known as the apical ectodermal ridge begins to elongate to form the apical ectodermal fold or finfold (Sordino and Duboule, 1996). This correlation between cessation of proliferation in the cellular populations fated to form the endoskeleton, formation of the finfold, and initiation of dermal fin skeleton development led to the hypothesis that a simple heterochronic shift in when ridge-fold transition takes place could explain the different skeletal morphologies seen in actinopterygians and sarcopterygians (Thorogood, 1991). There are two primary predictions based on this hypothesis. First, there will be a relative trade-off in the contribution of each skeletal type due to the necessary temporal segregation between endoskeletal proliferation and dermal ray formation. As a result, one should not see fin morphologies that consist of large endoskeletons *and* large dermal ray skeletons. Second, there should be little or no proximodistal overlap between the endoskeleton and the dermal rays unless the dermal rays were to extend or elongate proximally during development. The fins of *Sauripterus* demonstrate that these predictions do not hold true for all gnathostomes.

Polyodon and *Acipenser* are comparable to *Sauripterus* in possessing relatively elaborate, distalized endoskeletons *and* large dermal fin rays. Likewise, these Acipenseriformes feature a broad proximodistal zone of overlap between their dermal rays and the fin endoskeleton. At the earliest stages of finfold elongation (after ridge-fold transition) actinotrichia can be seen overlapping the distal margin of the endoskeletal disc (Fig. 3A,B). When the collagenous framework of the lepidotrichia first appears in *Polyodon* (37 days poststaging), this same relative degree of overlap with the radials is maintained (Fig. 3D). Distal radials begin to condense within the proximal finfold concomitant with lepidotrichial formation. Thus, the degree of overlap between the dermal fin skeleton and the proximal radials is determined at very early stages, with no evidence of subsequent migration or elongation of the dermal skeleton to overlap the radials. Furthermore, initiation of actinotrichial formation begins at Stage 42 in *Polyodon* and Stage 40 in *Acipenser*, shortly after initial elongation of the finfold (Stage 39 in *Polyodon*, Stage 38 in *Acipenser*) and prior to most of fin endoskeletal development. Thus, in contrast to the condition seen in teleosts, cessation of endoskeletal proliferation is not correlated with formation of the apical ectodermal fold in Acipenseriformes. These observations suggest that correlation of these two events in teleosts may represent a derived condition and that formation of the dermal rays and formation of the fin endoskeleton are neither temporally nor spatially segregated in all gnathostomes.

CONCLUSIONS

In both *Polyodon spathula* and *Acipenser transmontanus* different portions of the pectoral fin endoskeleton develop via two different mechanisms. In particular, there is a distinct difference between

the pattern of chondrogenesis of the metapterygium and the anterior radials. The anterior pectoral radials of Acipenseriformes, the propterygium and mesopterygial radials, are considered homologous to the pectoral radials of teleosts. As in teleosts, these elements develop by subdivision of an initially chondrogenic disc of cells. On the other hand, the Acipenseriform metapterygium is considered homologous to the monobasal fin skeleton of sarcopterygian fish and tetrapods. The metapterygium is initially continuous with the pectoral girdle in *Polyodon* and *Acipenser*; a condition similar to that described for the humerus and scapulocoracoid of the tetrapod *Ambystoma* (Burke, 1991). The metapterygium elongates in a proximal to distal direction through subsequent stages as metapterygial radials condense within the adjacent nonchondrogenic mesenchyme. Thus, the patterning mechanisms observed in the Acipenseriform fin reflects the putative homologies of respective elements based on fossil and morphological evidence. As such, the majority of extant osteichthyan diversity (i.e., teleosts and tetrapods) can be characterized by loss of different portions of the primitive developmental condition. In teleosts, the metapterygial axis is lost, resulting in a fin endoskeleton formed exclusively by the endoskeletal disc and the distal radials. Sarcopterygian fins have lost the endoskeletal disc and the distal radials, retaining only the metapterygial axis. These patterns of loss, in turn, may have allowed remaining skeletal structures to evolve in new ways. In tetrapods, evolutionary patterns of skeletal loss also include components of the dermal fin skeleton. Indeed, the loss of the paired fin lepidotrichia is a key novelty correlated with the origin of tetrapod limbs.

The patterns of variation seen in this study suggest a level of developmental independence between the formation of the anterior radials and the metapterygial axis. Such independence is supported by the convergent loss of anterior radials in fossil chondrichthyans and sarcopterygians and the loss of the metapterygium in teleosts. Likewise, basal gnathostome taxa vary in the number of endoskeletal radials anterior to the metapterygium, suggesting that variation in the pattern of endoskeletal disc subdivision may evolve without constraint on the metapterygium.

ACKNOWLEDGMENTS

Embryos of *Polyodon spathula* and invaluable technical support were provided by Steve Kahrs and the employees of Osage Catfisheries Inc., Osage Beach, Missouri. We thank Michael Coates, Victoria Prince, Melina Hale, Robert Ho, and members of their respective labs at the University of Chicago for assistance with ideas, techniques, and equipment. M.C.D. thanks William Bemis for sharing insights on, and his enthusiasm for, sturgeons and paddlefish. A.F. thanks John Postlethwait for support during sturgeon collection. The monoclonal antibody for type II collagen (II-II6B3) was originally developed by Thomas F. Linsenmayer of Tufts Medical School and was obtained from the Developmental Studies Hybridoma Bank under the auspices of the NICHD and maintained by the University of Iowa, Department of Biological Sciences.

LITERATURE CITED

Alberts B, Bray D, Lewis J, Raff M, Roberts K, Watson JD. 1983. Molecular biology of the cell. New York: Garland.

Balfour FM. 1881. On the development of the skeleton of the paired fins of Elasmobranchii, considered in relation to its bearings on the nature of the limbs of the Vertebrata. Proc Zool Soc Lond 1881:656–671.

Ballard WW, Needham RG. 1964. Normal embryonic stages of *Polyodon spathula* (Walbaum). J Morphol 114:465–478.

Bemis WE, Grande L. 1992. Early development of the Actinopterygian head. I. External development and staging of the paddlefish *Polyodon spathula*. J Morphol 213:47–83.

Bemis WE, Grande L. 1999. Development of the median fins of the North American paddlefish (*Polyodon spathula*), and a reevaluation of the lateral fin-fold hypothesis. In: Arratia G, Schultze H-P, editors. Mesozoic fishes 2—systematics and fossil record. Munich: Springer. p 41–68.

Bemis WE, Findeis EK, Grande L. 1997. An overview of Acipenseriformes. Environ Biol Fish 48:25–71.

Bouvet J. 1968. Histogenèse précoce et morphogenèse du squelette cartilagineux des ceintures primaraires et des nageoires paires chez la truite (*Salmo trutta fario* L.). Arch d'Anat Microsc 57:79–96.

Burke AC. 1991. Proximal elements in the vertebrate limb; evolutionary and developmental origin of the pectoral girdle. In: Hinchliffe JR, Hurle J, Summerbell D, editors. Developmental patterning of the vertebrate limb. NATO ASI Series A: Life Sciences, Vol. 205. London: Plenum Press. p 385–394.

Castagnola P, Dozin B, Moro G, Cancedda R. 1988. Changes in the expression of collagen genes show two stages in chondrocyte differentiation in vitro. J Cell Biol 106:461–467.

Coates MI. 1994. The origin of vertebrate limbs. In: Akam M, Holland P, Ingham P, Wray G, editors. The evolution of developmental mechanisms. Development 1994 (suppl):169–180.

Coates, MI. 1999. Endocranial preservation of a Carboniferous actinopterygian from Lancashire, U.K., and the interrelationships of primitive actinopterygians. Philos Trans R Soc B 354: 435–462.

Consi TR, Seifert PA, Triantafyllou MS, Edelman, ER. 2001. The dorsal fin engine of the seahorse (*Hippocampus sp*). J Morphol 248:80–97.

Davis MC. 2003. Chondrogenesis in the developing pectoral fins of the chondrosteans *Polyodon* and *Acipenser*. Abstracts of the 2003 Annual Meeting of the Society of Integrative and Comparative Biology. p 151A.

Davis MC, Shubin NH, Daeschler EB. 2001. Immature rhizodontids from the Devonian of North America. Bull Mus Comp Zool Harvard 155:665–681.

Davis MC, Shubin NH, Daeschler EB. 2004. A new specimen of *Sauripterus taylori* (Sarcopterygii, Osteichthyes) from the Famennian Catskill Formation of North America. J Vert Paleontol 24:26–40.

Denison R. 1978. Placodermi. In: Schultze H-P, editor. Handbook of paleoichthyology, vol. 2. New York: Gustav Fischer. p 1–128.

Denison R. 1979. Acanthodii. In: Schultze H-P, editor. Handbook of paleoichthyology, vol. 5. New York: Gustav Fischer. p 1–62.

De Pinna MCC. 1996. Teleostean monophyly. In: Stiassny MLJ, Parenti LR, Johnson GD, editors. Interrelationships of fishes. San Diego: Academic Press. p 147–162.

Detlaff TA, Ginsburg AS, Schmalhausen OI. 1993. Sturgeon fishes: developmental biology and aquaculture. Berlin: Springer.
Didier DA. 1995. Phylogenetic systematics of extant chimaeroid fishes (Holocephali, Chimaeroidei). Am Mus Novitates 3119:1–86.
Edwall-Arvidsson C, Wroblewski J. 1996. Characterization of chondrogenesis in cells isolated from limb buds in mouse. Anat Embryol (Berl) 193:453–461.
Findeis EK. 1997. Osteology and phylogenetic interrelationships of sturgeons (Acipenseridae). Environ Biol Fish 48:73–126.
Gardiner BG. 1984. The relationships of the palaeoniscid fishes, a review based on new specimens of *Mimia* and *Moythomsia* from the Upper Devonian of Western Australia. Bull Br Mus Nat Hist Geol 37:173–428.
Gardiner BG, Schaeffer B. 1989. Interrelationships of lower actinopterygian fishes. Zool J Linn Soc 97:135–187.
Gardiner BG, Maisey JG, Littlewood DTJ. 1996. Interrelationships of Basal Neopterygians. In: Stiassny M, Parenti L, Johnson GD, editors. Interrelationships of fishes. San Diego: Academic Press. p 117–146.
Gegenbaur C. 1865. Untersuchungen zur vergleichenden Anatomie der Wirbelthiere. Zweites Heft. Leipzig: Verlag von Wilhelm Engelmann.
Géraudie J. 1977. Initiation of the actinotrichial development in the early finbud of the fish, *Salmo*. J Morphol 151:353–362.
Géraudie J, Landis WJ. 1982. The fine structure of the developing pelvic fin dermal skeleton in the trout *Salmo gairdneri*. Am J Anat 163:141–156.
Goodrich ES. 1906. Notes on the development, structure and origin of the median and paired fins of fish. Q J Microsc Sci 50:333–376.
Grande L, Bemis WE. 1991. Osteology and phylogenetic relationships of fossil and recent paddlefish (Polyodontidae) with comments on the interrelationships of Acipenseriformes. J Vert Paleontol 11 (suppl 1):1–121.
Grande L, Bemis WE. 1996. Interrelationships of Acipenseriformes, with comments on "Chondrostei." In: Stiassny M, Parenti L, Johnson GD, editors. Interrelationships of fishes. San Diego: Academic Press. p 85–115.
Grande L, Jin F, Yabumoto Y, Bemis WE. 2002. *Protopsephurus liui*, a well preserved primitive paddlefish (Acipenseriformes: Polyodontidae) from the Lower Cretaceous of China. J Vert Paleontol 22:209–237.
Grandel H, Schulte-Merker S. 1998. The development of the paired fins in the Zebrafish (*Danio rerio*). Mech Dev 79:99–120.
Gross W. 1962. Neuuntersuchung der Stensiöellida (Arthrodira, Unterdevon). Notizbl Hess Landesamt Bodenf 89:17–43.
Hampe O, Heidtke UHJ. 1997. *Hagenoselache sippeli* n. gen. N. sp., ein früher xenacanthider Elasmobranchier aus dem Oberkarbon (Namurium B) von Hagen-Vorhalle (NW-Sauerland/Deutschland). Geol Paläont Westf 47:5–42.
Hilton EJ. 2002. Osteology of the extant North American fishes of the genus *Hiodon* Lesueur, 1818 (Teleostei: Osteoglossomorpha: Hiodontiformes). Fieldiana 100:1–142.
Inoue JG, Miya M, Tsukamoto K, Nishida M. 2003. Basal actinopterygian relationships: a mitogenomic perspective on the phylogeny of the "ancient fish." Mol Phylogenet Evol 26:110–120.
Janvier P. 1996. Early vertebrates. New York: Oxford University Press.
Jessen H. 1972. Schultergürtel und Pectoralflosse bei Actinopterygiern. Fossils Strata 1:1–101.
Jollie M. 1980. Development of head and pectoral girdle skeleton and scales in *Acipenser*. Copeia 1980:226–249.
Joss J, Longhurst T. 2001. Lungfish paired fins. In: Ahlberg PE, editor. Major events in early vertebrate evolution. New York: Taylor and Francis. p 370–376.
Kimura S, Uematsu Y, Miyauchi Y. 1986. Shark (*Prionace glauca*) elastoidin: characterization of its collagen as [alpha 1(E)]3 homotrimers. Comp Biochem Physiol B 84:305–308.
Kryzanovsky S. 1927. Die entwicklung der paarigen flossen bei *Acipenser, Amia* und *Lepidosteus*. Acta Zool 8:277–352.
Lê HLV, Lecointre G, Perasso R. 1993. A 28S rRNA-based phylogeny of the gnathostomes: First steps in the analysis of conflict and congruence with morphologically based cladograms. Mol Phylogenet Evol 2:31–51.
Long JA. 1988. New palaeoniscoid fishes from the Late Devonian and Early Carboniferous of Victoria. In: Jell PA, editor. Devonian and Carboniferous fish studies. Sydney: Association of Australasian Palaeontologists. p 1–64.
Mabee PM. 2000. Developmental data and phylogenetic systematics: evolution of the vertebrate limb. Am Zool 40:789–800.
Mabee PM, Trendler TA. 1996. Development of the cranium and paired fins in *Betta splendens* (Teleostei: Percomorpha): Intraspecific variation and interspecific comparisons. J Morphol 227:249–287.
Maisey JG. 1984. Chondrichthyan phylogeny: a look at the evidence. J Vert Paleontol 4:359–371.
Maisey JG. 1986. Heads and tails: a chordate phylogeny. Cladistics 2:201–256.
Mims SD, Shelton WL, Wynne FS, Onders RJ. 1999. Production of paddlefish. South Reg Aquacul Cent Pub 437.
Mina M, Kollar EJ, Upholt WB. 1991. Temporal and spatial expression of genes for cartilage extracellular matrix proteins during avian mandibular arch development. Differentiation 48: 17–24.
Mivart St.G. 1879. Notes on the fins of elasmobranchs, with considerations on the nature and homologies of the vertebrate limbs. Trans Zool Soc Lond 10:439–484.
Nelson GJ. 1969. Gill arches and the phylogeny of fishes, with notes on the classification of vertebrates. Bull Am Mus Nat Hist 141:475–552.
Ørvig T. 1962. Y a-t-il une relation directe entre les Arthrodires ptyctodontides et les Holocéphales? In: Lehman JP, editor. Problèmes actuels de paleontology: evolution des Vertébrés. Paris: Colloques internationaux du Centre national de la Recherche scientifique No. 104. p 49–61.
Patterson C. 1982. Morphology and interrelationships of primitive actinopterygian fishes. Am Zool 22:241–259.
Rabie ABM, She TT, Harley VR. 2003. Forward mandibular positioning up-regulates SOX9 and Type II collagen expression in the glenoid fossa. J Dent Res 82:725–730.
Robson P, Wright GM, Keeley FW. 2000. Distinct non-collagen based cartilages comprising the endoskeleton of the Atlantic hagfish, *Myxine glutinosa*. Anat Embryol 202:281–290.
Rodén L. 1980. Structure and metabolism of connective tissue proteoglycans. In: Lennarz WJ, editor. The biochemistry of glycoproteins and proteoglycans. New York: Plenum. p 267–371.
Schilling TF, Kimmel CB. 1997. Musculoskeletal patterning in the pharyngeal segments of the zebrafish embryo. Development 124:2945–2960.
Schmalhausen OI. 1991. The Russian sturgeon *Acipenser güldenstädti*. II. Later prelarval development. In: Dettlaff TA, Vassetzky SG, editors. Animal species for developmental studies, vol. 2. Vertebrates. New York: Consultants Bureau. p 67–88.
Semon R. 1898. Die Entwicklung der paarigen Flossen des *Ceratodus forsteri*. Jen Denkschr 4, Semon Zool Forschungsreisen 1:61–111.
Sewertzoff AN. 1926. Die morphologie der brustflossen der fishe. Jena Z Naturw 62:343–392.
Shubin N. 1995. The evolution of paired fins and the origin of tetrapod limbs—phylogenetic and transformational approaches. Evol Biol 28:39–86.
Shubin NH, Alberch P. 1986. A morphogenetic approach to the origin and basic organization of the tetrapod limb. Evol Biol 20:319–387.
Shubin NH, Davis MC. 2004. Modularity in the evolution of vertebrate appendages. In: Schlosser G, Wagner G, editors. Modularity in development and evolution. Chicago: University of Chicago Press. p 429–440.
Sordino PF, Duboule D. 1996. A molecular approach to the evolution of vertebrate paired appendages. Trends Evol Ecol 11: 114–119.

Stahl BJ. 1999. Chondrichthyes III: Holocephali. In: Schultze H-P editor. Handbook of paleoichthyology. New York: Gustav Fischer. p 1–164.

Takahashi I, Nuckolls GH, Takahashi K, Tananka O, Semba I, Dashner R, Shum L, Slavkin HC. 1998. Compressive force promotes sox9, type II collagen and aggrecan and inhibits IL-1beta expression resulting in chondrogenesis in mouse embryonic limb bud mesenchymal cells. J Cell Sci 111:2067–2076.

Thacher JK. 1877. Median and paired fins, a contribution to the history of the vertebrate limbs. Trans Conn Acad 3:281–310.

Thorogood P. 1991. The development of the teleost fin and implications for our understanding of tetrapod limb evolution. In: Hinchliffe JR, Hurle J, Summerbell D, editors. Developmental patterning of the vertebrate limb. NATO ASI Series A: Life Sciences, Vol. 205. London: Plenum Press. p 347–354.

Venkatesh B, Erdmann MV, Brenner S. 2001. Molecular synapomorphies resolve evolutionary relationships of extant jawed vertebrates. Proc Natl Acad Sci U S A 98:11382–11387.

Wake DB, Shubin N. 1998. Limb development in the pacific giant salamanders, *Dicamptodon* (Amphibia, Caudata, Dicamptodontidae). Can J Zool 76:2058–2066.

Westerfield M. 2000. The zebrafish book. A guide for the laboratory use of zebrafish (*Danio rerio*), 4th ed. Eugene: University of Oregon Press.

Wood A. 1982. Early pectoral fin development and morphogenesis of the apical ectodermal ridge in the Killifish, *Aphyosemion scheeli*. Anat Rec 204:349–356.

Wood A, Thorogood P. 1984. An analysis of in vivo cell migration during teleost fin morphogenesis. J Cell Sci 66:205–222.

Yan YL, Miller CT, Nissen RM, Singer A, Liu D, Kirn A, Draper B, Willoughby J, Morcos PA, Amsterdam A, Chung BC, Westerfield M, Haffter P, Hopkins N, Kimmel C, Postlethwait JH, Nissen RM. 2002. A zebrafish sox9 gene required for cartilage morphogenesis. Development 129:5065–5079.

Zangerl R. 1981. Chondrichthyes. I. Paleozoic Elasmobranchii. In: Schultze H-P, editor. Handbook of paleoichthyology, vol. 3A. New York: Gustav Fischer. p 115.